2023 DRAFT COASTAL MASTER PLAN

2023 BARRIER ISLAND MODEL: ICM-BITI AND ICM-BI

ATTACHMENT C9

REPORT: VERSION 02
DATE: FEBRUARY 2021
PREPARED BY: SOUPY DALYANDER, MADELINE FOSTER-MARTINEZ, DIANA DI LEONARDO, IOANNIS GEORGIOU, MICHAEL MINER, CATHERINE FITZPATRICK

COASTAL PROTECTION AND RESTORATION AUTHORITY
150 TERRACE AVENUE
BATON ROUGE, LA 70802
WWW.COASTAL.LA.GOV

COASTAL PROTECTION AND RESTORATION AUTHORITY

This document was developed in support of the 2023 Coastal Master Plan being prepared by the Coastal Protection and Restoration Authority (CPRA). CPRA was established by the Louisiana Legislature in response to Hurricanes Katrina and Rita through Act 8 of the First Extraordinary Session of 2005. Act 8 of the First Extraordinary Session of 2005 expanded the membership, duties, and responsibilities of CPRA and charged the new authority to develop and implement a comprehensive coastal protection plan, consisting of a master plan (revised every six years) and annual plans. CPRA's mandate is to develop, implement, and enforce a comprehensive coastal protection and restoration master plan.

CITATION

Dalyander, S., Foster-Martinez, M., Di Leonardo, D., Georgiou, I. Y., Miner, M.D., Fitzpatrick, C. E. (2020). 2023 Draft Coastal Master Plan Louisiana Coastal Master Plan 2023 Barrier Island Model: ICM-BITI and ICM-BI. Version 2. (p. 70). Baton Rouge, Louisiana: Coastal Protection and Restoration Authority.

ACKNOWLEDGEMENTS

This document was developed as part of a broader Model Improvement Plan in support of the 2023 Coastal Master Plan under the guidance of the Modeling Decision Team (MDT):

- Coastal Protection and Restoration Authority (CPRA) of Louisiana – Elizabeth Jarrell, Stuart Brown, Ashley Cobb, Catherine Fitzpatrick, Krista Jankowski, David Lindquist, Sam Martin, and Eric White
- University of New Orleans – Denise Reed

This document was prepared by the 2023 Coastal Master Plan Barrier Island Team:

- Ioannis Georgiou – The Water Institute of the Gulf
- Catherine Fitzpatrick – CPRA
- Soupy Dalyander – The Water Institute of the Gulf
- Maddie Foster-Martinez – University of New Orleans
- Diana Di Leonardo – The Water Institute of the Gulf
- Mike Miner – The Water Institute of the Gulf

The team would like to thank Zhifei Dong, with APTIM, Inc. and Ben Beasley and Mark Byrnes with Applied Coastal Research and Engineering, Inc. for their valuable input on these recommended improvements.

EXECUTIVE SUMMARY

The 2023 Coastal Master Plan relies on realistic predictive modeling of the migration of coastal barrier islands and their effect on coastal basin hydrology, while incorporating periodic maintenance of barrier islands via assumed restoration. The ICM-Barrier Islands Improvement Team was tasked with recommending improvements to the 2017 Barrier Island Model (BIMODE), which were shared in a 2019 Technical Report (Georgiou et al., 2019). Two main priorities were highlighted in the technical report, and as a result barrier islands will be considered within the 2023 Integrated Compartment Model (ICM) using two separate modules: the Barrier Island Tidal Inlet Module (BITI), which models the evolution of tidal inlets along barrier islands as informed by basin hydraulics, and the Barrier Island Digital Elevation Model (ICM-BI), which models island configuration through time to support storm surge modeling. The BITI module is fully incorporated in the ICM, while ICM-BI informs the model at various time steps.

The BITI module captures the positive relationship between tidal inlet cross sectional area and back barrier tidal prism. It uses the O'Brien-Jarrett-Marchi law to calculate an inlet's cross sectional area using the basin's tidal prism. Due to the size of each coastal basin and the presence of multiple barrier island tidal inlets per basin, BITI calculates a fraction of the total tidal prism as it pertains to each tidal inlet using a partitioning coefficient. The module has the capability to evolve inlets as the size of the back barrier basin and tidal prism increases over time and ICM-Hydro compartments convert to open water.

The second module, ICM-BI, has several key components. It uses historic barrier island cross-shore retreat rates from three sources (Beasley et al. 2018, 2019, and the Barrier Island Comprehensive Monitoring program, or BICM) under varying sea level rise (SLR) scenarios to migrate barrier island transects. The transects migrate based on cross-shore retreat rates of index profiles selected to represent key geomorphic features along the coast. The second component of ICM-BI is the auto-restoration feature. This feature reflects the assumption that CPRA will maintain the integrity of the barrier island system through the Barrier Island System Management (BISM) program. In line with BISM, master plan predictive modeling efforts define barrier island integrity as preventing and repairing breaches and maintaining a critical width for each island. The auto-restoration feature represents this assumption by placing sediment on restoration units that drop below a critical width threshold. ICM-BI, after running the various components of the module passes a new DEM to the ICM and ADCIRC models at an annual time step.

TABLE OF CONTENTS

LIST OF TABLES

LIST OF FIGURES

LIST OF ABBREVIATIONS

BICM ..... BARRIER ISLAND COMPREHENSIVE MONITORING PROGRAM
BIMODE ..... (2017 COASTAL MASTER PLAN) BARRIER ISLAND MODEL DEVELOPMENT
BISM ..... BARRIER ISLAND SYSTEM MANAGEMENT
BITI ..... BARRIER ISLAND TIDAL INLET MODULE
BRIE ..... BARRIER ISLAND AND INLET ENVIRONMENT MODEL
CPRA ..... COASTAL PROTECTION AND RESTORATION AUTHORITY
CRMS ..... COASTWIDE REFERENCE MONITORING SYSTEM
DEM ..... DIGITAL ELEVATION MODEL
HWS ..... HIGH WATER SLACK
I/0 ..... INPUT/OUTPUT
ICM ..... INTEGRATED COMPARTMENT MODEL
ICM BI ..... ICM BARRIER ISLAND DIGITAL ELEVATION MODEL
LAVEGMOD ..... LOUISIANA VEGETATION MODULE
LWS ..... LOW WATER SLACK
MDT ..... MODEL DECISION TEAM
MHW ..... MEAN HIGH WATER
MSL ..... MEAN SEA LEVEL
NOAA ..... NATIONAL OCEANIC AND ATMOSPHERIC ADMINISTRATION
NGOM2DEM ..... NORTHERN GULF OF MEXICO DEM
PM-TAC ..... PREDICTIVE MODEL TECHNICAL ADVISORY COMMITTEE
RSLR ..... RELATIVE SEA LEVEL RISE
SLR ..... SEA LEVEL RISE
SSH ..... SEA SURFACE HEIGHT
USGS ..... UNITED STATES GEOLOGICAL SURVEY

1.0 INTRODUCTION

This report summarizes the barrier island digital elevation model (ICM-BI) and the Barrier Island Tidal Inlet (ICM-BITI) module for the 2023 Coastal Master Plan. Updates were made to the 2017 Barrier Island Model Development (BIMODE) framework (Poff et al., 2017), and changes represent the implementation of recommendations made in a July 31, 2019 technical report by the ICM-Barrier Islands Improvement Team (Georgiou et al., 2019). Georgiou et al. (2019) highlighted two main requirements for the modeling of barrier islands and associated dynamics within the Integrated Compartment Model (ICM): 1) simulate coastal barrier island hydraulics that inform the ICM basin hydraulics with feedback between the two, and 2) predict barrier island evolution to provide future (e.g., at least 50 years) morphology configurations to support storm surge modeling. This report summarizes the subroutine that addresses these objectives, with ICM-BITI informing changes to basin hydraulics and ICM-BI predicting barrier island and headland morphology change.

2.0 BARRIER ISLAND TIDAL INLET (BITI) MODULE

2.1 INTRODUCTION

Tidal inlets comprise an important component of the barrier and overall estuarine system by facilitating water, sediment, and nutrient exchange between the back-barrier environment and coastal ocean (FitzGerald & Miner, 2013; Ranasinghe et al., 2013). Inlet size is controlled by tidal currents that remove wave-deposited sand and lead to the development of ebb- and flood- deltas seaward and landward of the inlet throat, respectively (FitzGerald et al., 1984; Hayes, 1980). The volume of water that moves through the inlet over a tidal cycle is called the tidal prism, while the tidal range is the vertical difference between high and low tide. O'Brien (1966) reported that inlet cross-sectional area is positively correlated to the tidal prism, a finding also supported by Jarrett (1976) and D'Alpaos et al. (2009). Walton and Adams (1976) reported that the volume of sand comprising the ebb tidal delta also correlates with the tidal prism. Increasing water levels in the basin reduce frictional damping of the tidal wave, thus increasing the back-barrier tidal range, which further augments the tidal prism (Gehrels et al., 1995; Howes, 2009). Therefore, loss of interior wetlands increases tidal prism and facilitates enlargement of the ebb delta and the inlet throat (FitzGerald et al., 2007; Miner et al., 2009a). The 2023 Barrier Island Tidal Inlet (BITI) module captures dynamic inlet throat geometry by changing the inlet cross-sectional area informed by changes in basin tidal prism.

2.2 MODULE DEVELOPMENT

The BITI module is a part of the ICM and is independent from ICM-BI. BITI calculates changes in the cross-sectional area of inlets, which are represented in ICM-Hydro as Type 1 links between compartments (McCorquodale et al., 2017). The 2012 Coastal Master Plan included a tidal inlet model, which computed an increase in tidal inlet cross-sectional area resulting from an increase in the tidal prism in the back-barrier basins once every 25 model years (Hughes et al., 2012). This model was not active for the 2017 Coastal Master Plan. For the 2023 Coastal Master Plan, the inlet module was improved from the 2012 version and incorporated within the ICM Python code.

BASIN HYDRO COMPARTMENTS

Obtaining an accurate tidal prism value requires the delineation of the ICM-Hydro compartments that contribute to a basin's tidal prism (

Figure 1); the tidal prism associated with each of those compartments (outlined in orange) is calculated by ICM-Hydro, whereas the compartment outlined in blue is not initially included. Over time, as the compartment outlined in blue gradually converts to open water, ICM-Hydro will consider this compartment in tidal prism calculations. Total tidal prism for the basin is calculated as follows:

$$\sum_{i=1}^{n} A_{w,i} T_i = P \quad (1)$$

Where

$\mathrm{P} =$ total tidal prism (m^3) of the basin

$T =$ mean spring tidal range (m) for the i^{th} ICM-Hydro compartment in the basin

$A_w =$ area (m^2) of open water of the i^{th} ICM-Hydro compartment in the basin

n = total number of ICM-Hydro compartments in the basin

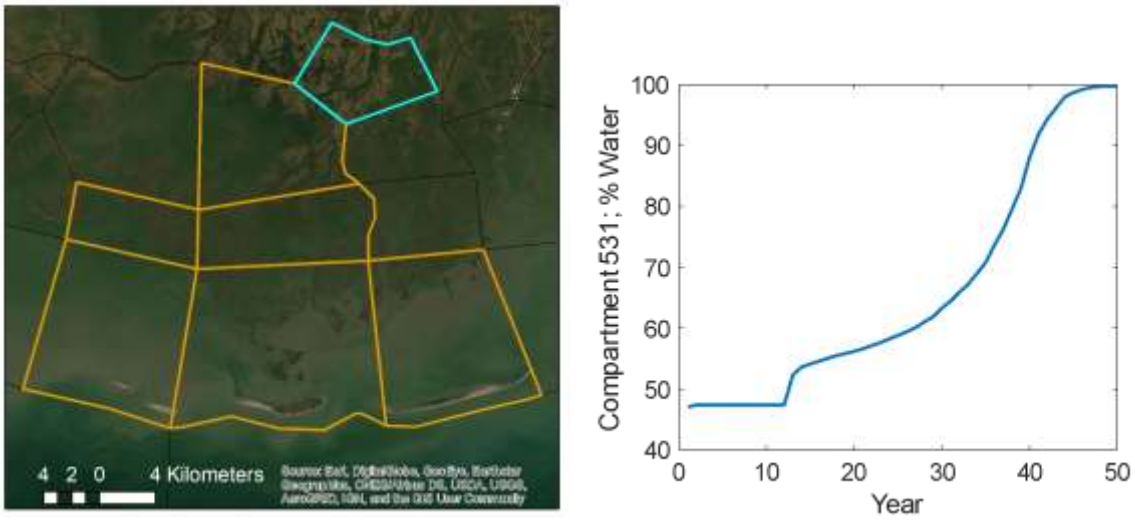

Figure 1. Left: Map of ICM-Hydro compartments from the 2017 Coastal Master Plan ICM for the Isles Dernieres Barrier Islands, used for illustrative purposes. ICM-Hydro compartments outlined in orange were designated as part of the basin and contributed to the tidal prism calculation. The ICM-Hydro compartment outlined in blue, Compartment 531, was not initially designated as part of the basin. Right: Results from the 2017 Coastal Master Plan for Compartment 531. The percent of the area that is open water increases over time. By year 50, the compartment is 100% open water.

Estuaries experience tidal variations. However, their upper reaches, where estuaries transition to swamps, coastal forests and tributaries may experience little to no tidal variation. As a result, as wetlands, swamps, and other landscapes convert to open water, the tidal prism would increase were these now open water areas to become tidal. For the 2017 Coastal Master Plan Barrier Island model, the ICM-Hydro compartments that make up each basin were predefined, limited in spatial extent, and did not change through time. As land converts to open water, more compartments need to be included for an accurate tidal prism calculation (example shown in

Figure 1). To avoid this issue, all ICM-Hydro compartments from “ridge-to-ridge” of each basin are included as contributors to the basin tidal prism in the BITI model, including ICM-Hydro compartments that are majority non-water (Figure 2). Initially, the non-water ICM-Hydro compartments have negligible contributions to the tidal prism, but as open water is created, their contribution increases. For basins not completely bound by land, the boundary was set as the last ICM-Hydro compartment containing an inlet link.

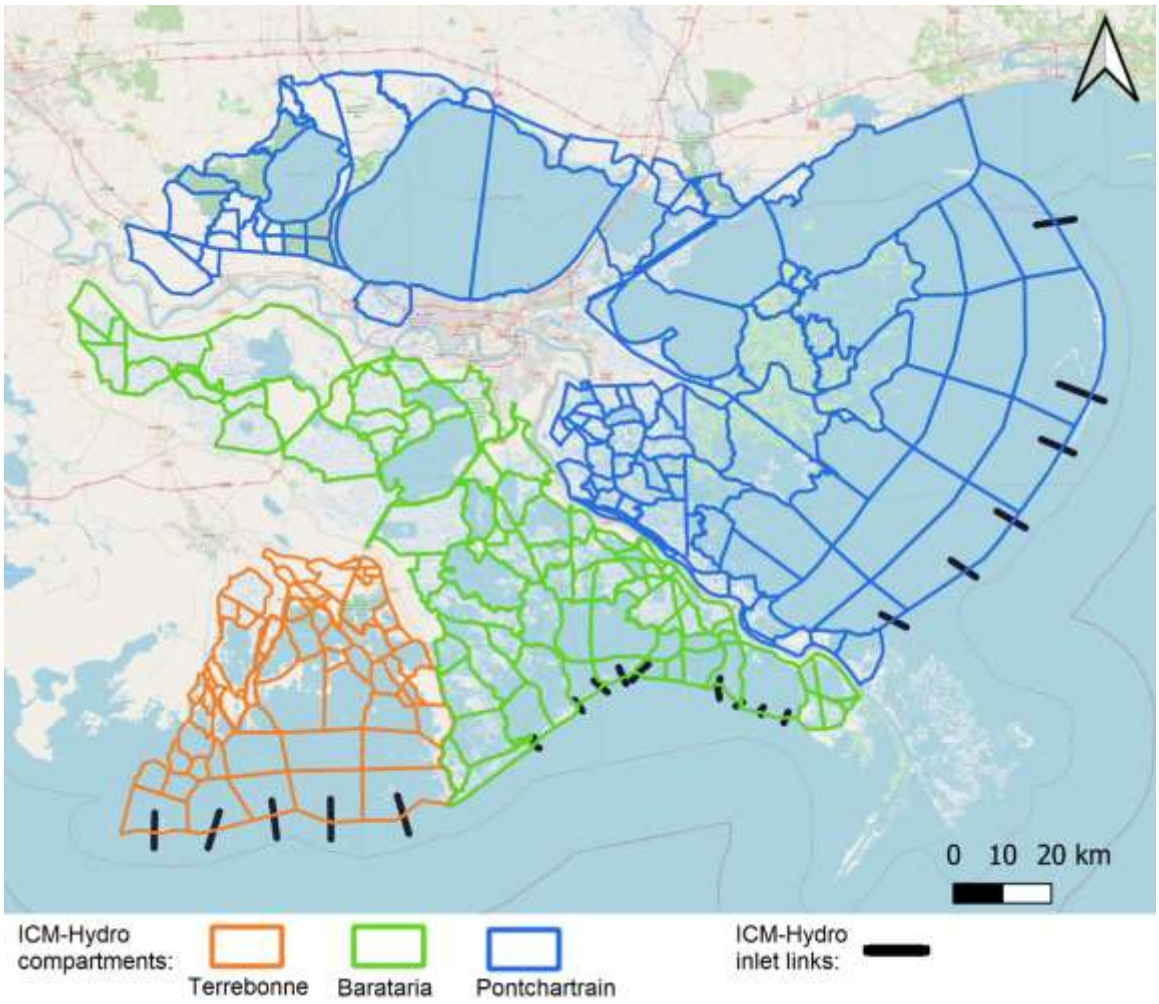

Figure 2. Map of the BITI domain.

TIDAL ATTENUATION

Tidal attenuation causes a phase lag in the tidal signal as it propagates in the estuary. Depending on the geometry and connectivity of the basin, this lag can cause the upper and lower parts of the basin to be out of phase. When lag times in diurnal systems between the upper and lower estuary are more than half the period of the diurnal tide (~12 hours), the resulting tidal prism would be smaller compared to a basin with lag times less than 12 hours. For example, tidal attenuation associated with channels in the Barataria Basin (e.g., Bayou Rigolets, Little Lake; Figure 3) inhibits connectivity between the lower and upper basin. Examining the sea surface height over a tidal cycle shows that the areas beyond 55 km up-basin (near Lake Salvador, Figure 4) from Barataria Pass are out of phase

with the lower basin. The net change in this upper part of the basin is in the opposite direction (i.e., instead of emptying toward the inlet some of water is drawn “up-basin”) and does not contribute to the total basin tidal prism (Howes, 2009).

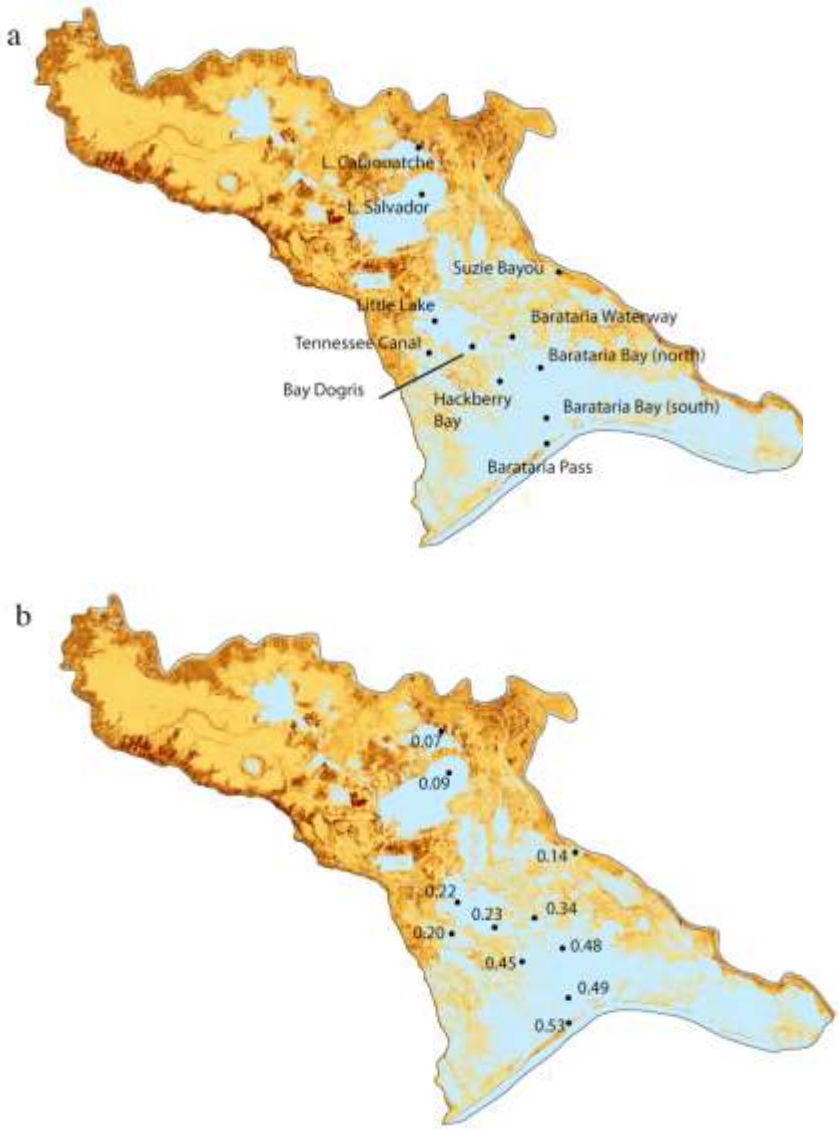

Figure 3. United States Geological Survey (USGS) water level gauges in the Barataria Basin (a). Tidal range in meters at each USGS gauge (b). Note the reduced tidal range in an up-basin direction. Figure from Howes (2009).

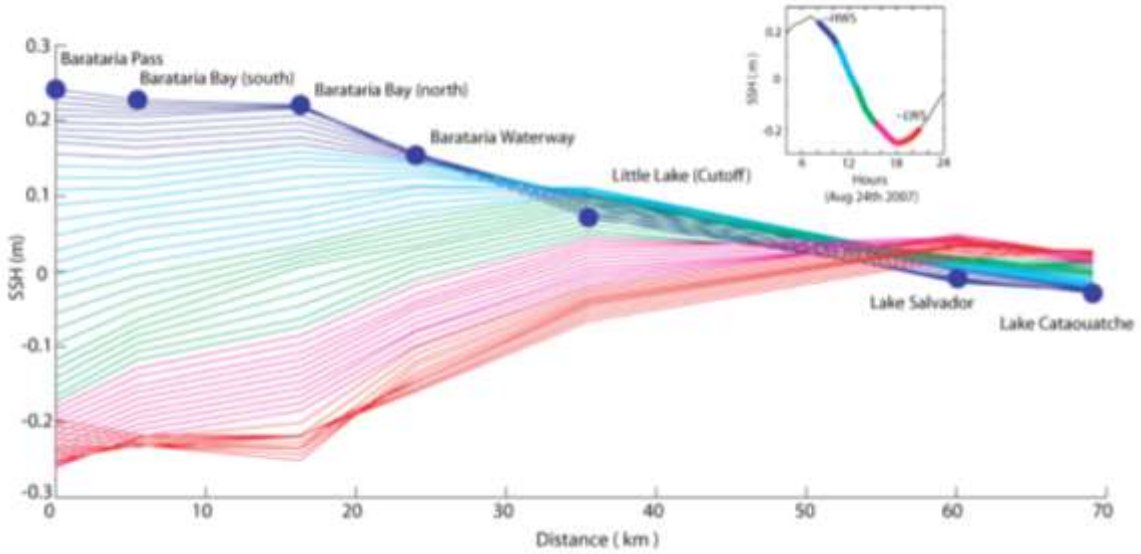

Figure 4. Isochrons, or snapshots through time, of sea surface height (SSH) over the length of Barataria Basin between high water slack (HWS) and low water slack (LWS). The color of the line corresponds to the color of the tidal stage shown in the inset in the upper right-hand corner (e.g., dark blue is HWS). It is a net change in water surface that contributes to tidal prism for the cycle. Lakes Salvador and Cataouatche are out of phase with respect to the rest of the basin. Figure from Howes (2009).

Tidal attenuation was considered during the calibration and validation phase because calibrated ICM-Hydro results were used. The hourly stage data used for this analysis, while not from the final calibrated ICM-Hydro model, was from a simulation in which the regional 2D ICM-Hydro models had been calibrated for stage and flows prior to the complete coupling with the 1D channel routing subroutines. ICM-Hydro was calibrated using a network of water level gauges through all basins operated by various organizations and agencies (e.g., USGS, National Oceanic and Atmospheric Association [NOAA], Coastwide Reference Monitoring System [CRMS]; White et al., 2017). Isochrons, or snapshots through time (Figure 4), were constructed to examine the presence or absence of—and the degree to which—tidal attenuation alters basin tidal dynamics.

EFFECTIVE TIDAL PRISM

The O'Brien-Jarrett-Marchi law (D'Alpaos et al., 2009) can be used to find the minimum (equilibrium) cross-sectional area of an inlet given the basin tidal prism:

$$A_I = kP^a \quad (2)$$

Where

$A_I =$ inlet cross-sectional area

$k =$ regional scale coefficient for the Gulf of Mexico (un-jettied inlets)

$P =$ total tidal prism for the basin

$a =$ regional scale exponent for the Gulf of Mexico (un-jettied inlets)

Within the Louisiana barrier island system, there is more than one inlet per basin, meaning that the cumulative cross-sectional flow area is distributed across multiple inlets. For the 2012 Coastal Master Plan, any increase in cross-sectional inlet area was equally distributed between the inlets connected to a basin. This approach led to instances where localized land loss unrealistically drove regional increases in inlet cross-sectional area, or conversely, where spatially variant land loss led to equal distribution of inlet cross-sectional area change across proximate and distal inlets. Instead, an increase in tidal prism should contribute to an increase in the specific inlets that convey the additional volume.

A more realistic representation is achieved by using an effective tidal prism volume for each inlet. The effective tidal prism is the volume of water conveyed through one inlet over a tidal cycle (for back-barrier systems with multiple inlets); it is a fraction of the total tidal prism for the basin. The total tidal prism for the basin is the sum of the effective tidal prisms for all basin inlets. For the 2023 Coastal Master Plan, the effective tidal prism is calculated by using partitioning coefficients for each ICM-Hydro compartment. The partitioning coefficient is the portion of the tidal prism in one ICM-Hydro compartment that is conveyed through a particular inlet. All Type 1 links that connect the ICM-Hydro

compartments within each basin to the Gulf of Mexico are designated as inlet links (McCorquodale et al., 2017). Each ICM-Hydro compartment has m partitioning coefficients, where m is the number of links in the basin, and the partitioning coefficients sum to one, as follows:

$$\sum_{i=1}^{m} p_i = 1 \quad (3)$$

Where

$p =$ partitioning coefficient, the fraction of the tidal prism in an ICM-Hydro compartment that is conveyed through a link

$m =$ the total number of links that convey flow in a basin

The p values vary from 0 to 1; they are predetermined for each ICM-Hydro compartment and do not change over time. Using the partitioning coefficients, the effective tidal prism for a link (example shown for Link A) is defined as:

$$\sum_{i=1}^{n} A_{w,i} T_i p_{A,i} = P_A \quad (4)$$

Where

$P_A =$ tidal prism (m^3) of the basin conveyed through Inlet A

$T =$ mean spring tidal range (m) for the ICM-Hydro compartment in the basin

$A_w =$ area (m^2) of open water of the ICM-Hydro compartment in the basin

$p =$ partitioning coefficient, the fraction of the tidal prism in the ICM-Hydro compartment that is conveyed through Inlet A

$n =$ the number of ICM-Hydro compartments which make up a given basin

Figure 5 illustrates a basin with four links (yellow and black lines). Each ICM-Hydro compartment has four partitioning coefficients that correspond to each link (shown by corresponding colors). For example, Link #1 (red, first number in each list) receives 100% and 10% of the tidal prism from the two left-most ICM-Hydro compartments and none of the tidal prism from the three right-most ICM-Hydro compartments. Partitioning coefficients are only displayed for a subset of compartments, but all compartments in the basin are assigned coefficients.

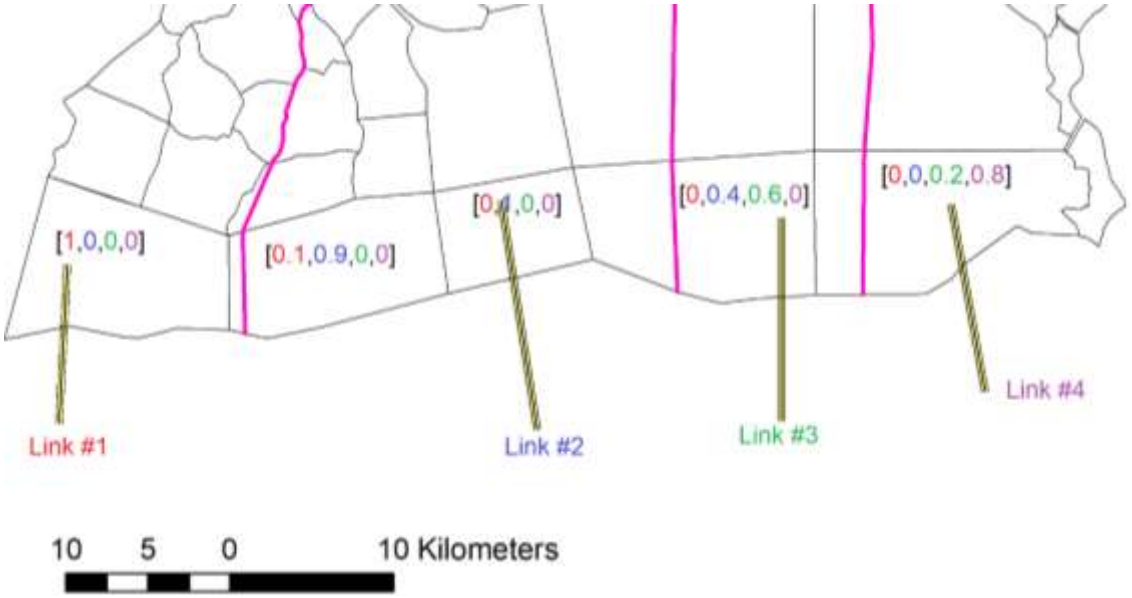

Figure 5. Example of partitioning coefficients in a basin. This basin has four inlets, represented by the four links (yellow and black lines). The basin area is divided (pink lines) between the links. The area between the pink lines is the portion of the basin's tidal prism conveyed through that link. Each ICM-Hydro compartment has a partitioning coefficient for each link (shown by corresponding colors).

DETERMINING PARTITIONING COEFFICIENTS

Partitioning coefficients were determined during the calibration and validation phase with the 2023 ICM-Hydro compartments and links. An initial partitioning of each basin (i.e., pink lines in Figure 5) was based on the size and proximity of each ICM-Hydro compartment-link pair, as well as natural hydrologic divides and known flow paths (i.e., bayous, channels). This allocates a fraction of the basin area to each link. For ICM-Hydro compartments at distance from the links or where hydrologic divides were not readily apparent, the contributions of each ICM-Hydro compartment were adjusted until the total tidal prism to inlet cross-sectional area was constant across the entire basin. This process is

described in further detail in the Partitioning Coefficients section of this report.

INLET LINKS

The cross-sectional areas for inlet links are updated with the changes in tidal prism. Dormant links, used in the 2017 Coastal Master Plan to allow for the possibility of island breaching, are not considered. This approach is consistent with the underlying assumption that the Barrier Island System Management (BISM) program will maintain barrier island integrity over time (i.e., prevent or repair breaching that would result in hydraulic connectivity through a previously contiguous barrier island).

LINK ATTRIBUTES

The output of the O'Brien-Jarrett-Marchi law (D'Alpaos et al., 2009) is an inlet channel cross-sectional area, but the ICM links are described with attributes of width and depth. To convert the area to width and depth, an aspect ratio was assigned to every link. The aspect ratio dictates how a change in area is distributed across width and depth. Previous studies have shown that inlet morphology in Louisiana is variable (Levin, 1993; Kindinger et al., 2013); some inlets have incised, while others have developed broad shoals (Figure 6; Miner et al., 2009a). Existing aspect ratios were used and were kept constant in time because the available historical data (Figure 6; Miner et al., 2009a) show that the aspect ratio does not change appreciably over time. Hence, the inlet aspect ratios were used as follows to distribute the link area:

$$\frac{W}{d} = r \quad (5)$$

$$A_I = W * d = rd * d \quad (6)$$

Where

$r =$ aspect ratio for inlet shape

$W =$ width of the tidal inlet (m)

$d =$ depth of the tidal inlet (m)

$A_I =$ inlet cross-sectional area (m^2)

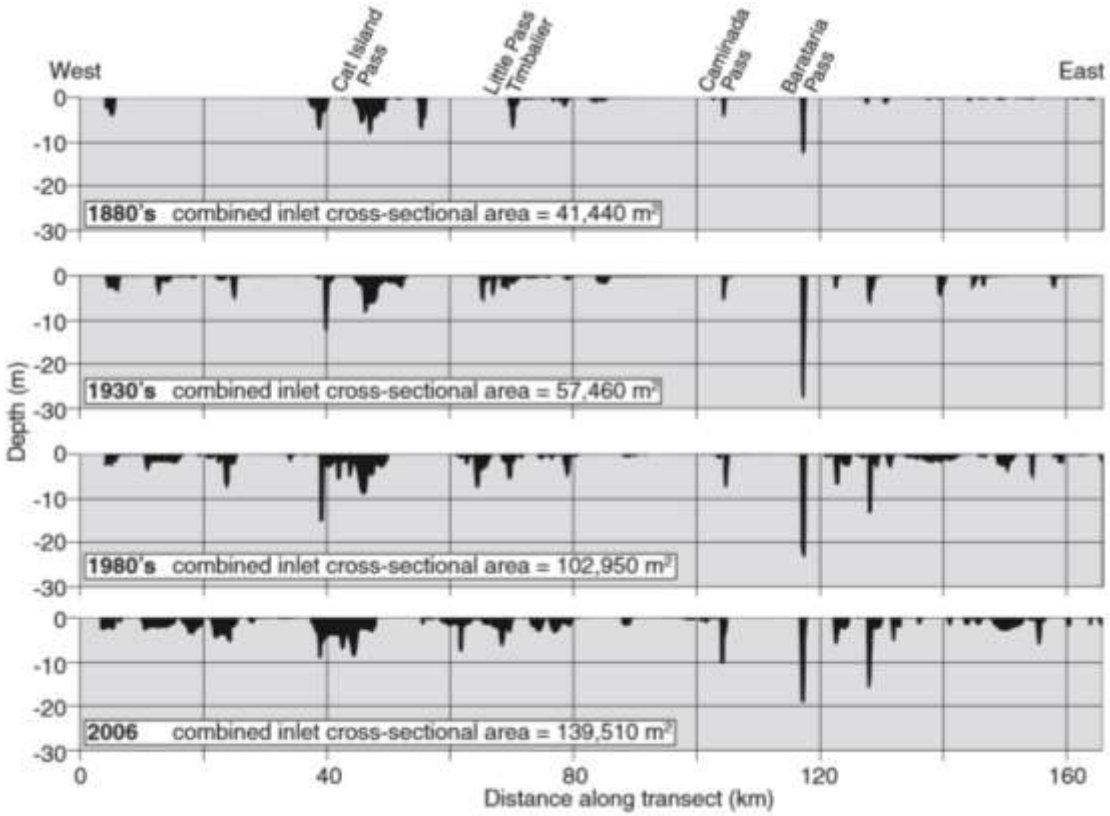

Figure 6. Historical trends in tidal inlet cross-sectional area for Raccoon Point to Sandy Point (1880–2006). Profiles trend along the barrier shoreline and intersect inlets at the location of minimum throat cross-sectional area for each time period. Note the widening and deepening at existing inlets as additional, stable inlets simultaneously form, resulting in a >threefold increase in combined cross-sectional area during the 125 years in response to an increasing tidal prism, while inlet aspect ratios remain relatively constant. The 1880s to 1980s bathymetry is from List et al. (1994). From Miner et al. (2009a).

2.3 CALIBRATION AND VALIDATION

The BITI module was calibrated to produce the existing 2023 ICM-Hydro inlet dimensions. We chose to retain these inlet dimensions for three reasons:

1) The ICM-Hydro inlet links are somewhat idealized. They are perfectly rectangular and, in a few

locations, represent a combination of multiple smaller inlets. Therefore, bathymetry measurements would need to be adjusted to fit this framework.

2) Where bathymetry data were available, the ICM-Hydro inlet link dimensions were a good cross-sectional representation of the inlet (Figure 7).

3) Maintaining existing dimensions minimized interference in the ICM-Hydro calibration and validation process.

The following sections describe how the BITI parameters were calibrated to the ICM-Hydro inlet link dimensions, as well as the calibration and validation process for tidal attenuation.

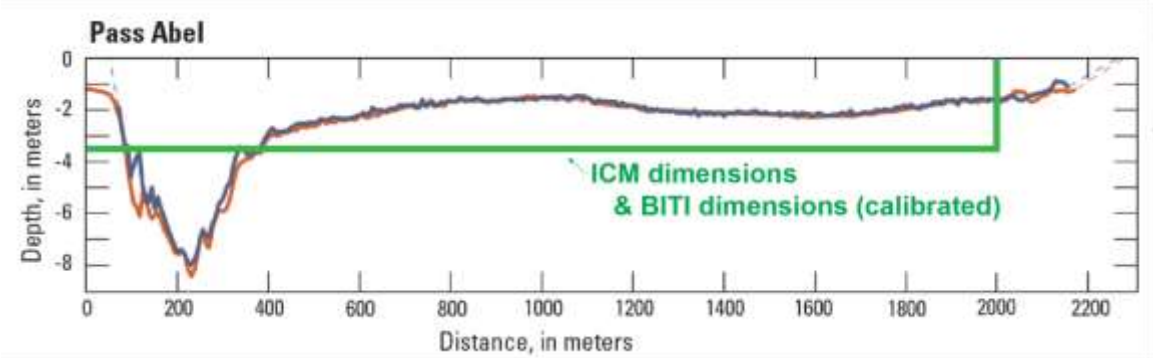

Figure 7. Comparison of measured bathymetry of Pass Abel and the ICM-Hydro inlet link dimensions for Pass Abel. Base figure is from Kindinger et al. (2013), and the green overlay was added.

TIDAL ATTENUATION

Hourly data were obtained from ICM-Hydro output for year 2014 to construct water level isochrons. Tidal attenuation was observed as tidal range decreased up-basin, but a phase lag was not observed (Figure 8). The absence of phase lag simplified the process of selecting ICM-Hydro compartments to be included in the tidal prism calculation. Rather than exclude compartments based on location, compartments are excluded if the annual mean of the daily tidal range is less than 0.10 m (Figure 9). This threshold distinguished well between tidal and sub-tidal water level fluctuations. Using this threshold, the ICM-Hydro compartments removed from the tidal prism calculation in Barataria Sound Basin align well with the contributions to the tidal prism observed by Howes (2009) and shown in Figure 3 and Figure 8.

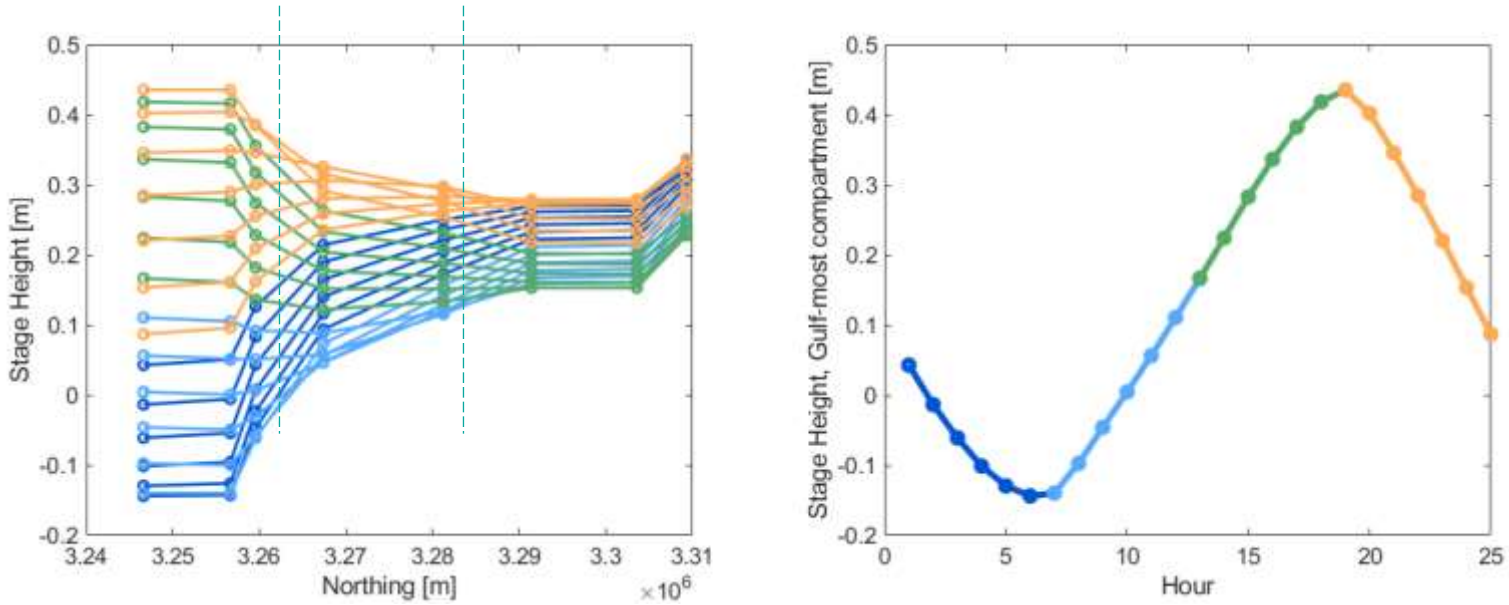

Figure 8. Right: Hourly isochrons of stage height over a 24-hour period in ICM-Hydro compartments from Barataria Pass moving up-estuary. Data is from a 2017 ICM-Hydro run. ICM-Hydro compartments are shown at the Northing coordinate of their centroid location. Moving from left to right, the first dashed black line is the location of the Little Lake compartment, and the second is the Lake Salvador compartment. Left: Stage height at the Barataria Pass compartment. Colors in the left panel match the time period of the colors in the right panel.

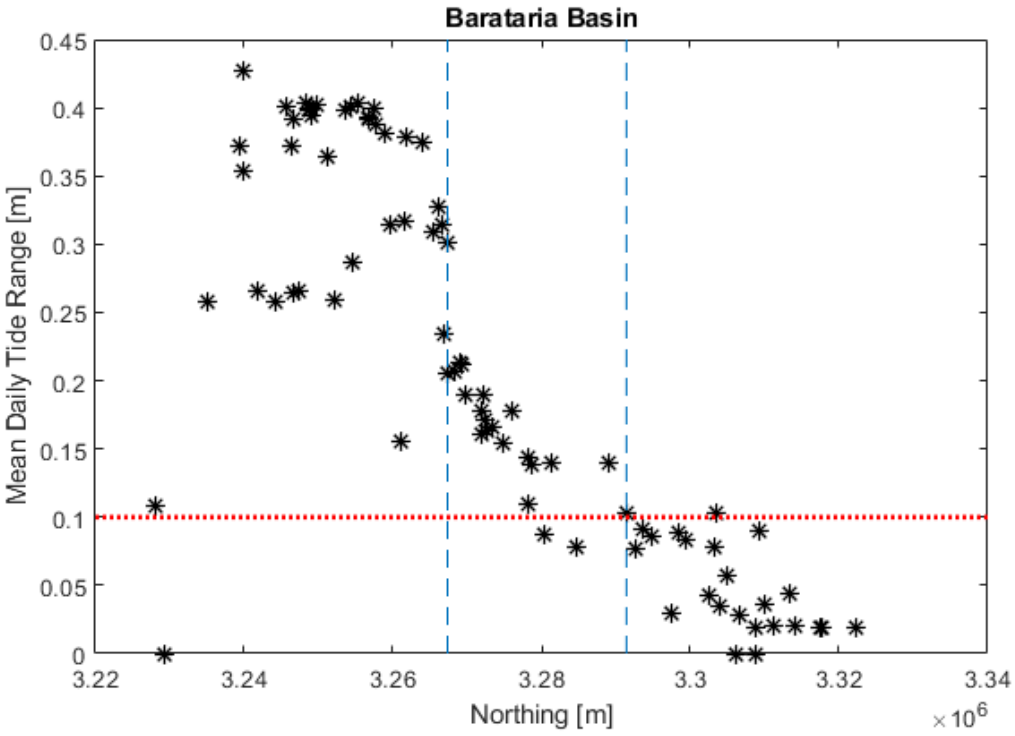

Figure 9. The annual mean daily tide range for each ICM-Hydro compartment in Barataria Basin considered in the tidal prism calculation. ICM-Hydro compartments are shown at the Northing coordinate of their centroid location. Moving from left to right, the first dashed blue line is the location of the Little Lake compartment, and the second is the Lake Salvador compartment.

PARTITIONING COEFFICIENTS

To calibrate the partitioning coefficients, the total inlet area across each basin was calculated using the basin wide tidal prism and the O'Brien-Jarrett-Marchi law (Eq. 2). This value was then compared to the total found by summing the ICM-Hydro inlet link areas. For each basin, the ICM-Hydro inlet link areas were greater than those calculated using the tidal prism and the O'Brien-Jarrett-Marchi law (Figure 10). These predicted inlet areas differ, in part because the annual average tidal range was used in the tidal prism calculation, instead of the spring tide range, which yields a smaller tidal prism and thus a smaller inlet area. The implementation of the average tidal range calculation within the ICM is simpler and more representative compared to using the maximum tidal range. This is due to the influence of other, non-tidal processes (e.g., storms) on the maximum tidal range. Additionally, the O'Brien-Jarrett-Marchi law assumes the system is in morphodynamic equilibrium. The ratio of these

two areas, or the basin wide factor, contains complexity arising from both influences—in addition to the modeling uncertainty—and indicates how far out of equilibrium the system is (assuming validity of the O'Brien-Jarrett-Marchi equilibrium assumption). The values for each basin are found in Table 1.

Table 1. The basin wide factors for each of the three basins.

Basin	Basin Wide Factor = $\frac{A_{ICM-Hydro\ \ inlet\ \ link}}{A_{O'Brien-Jarrett-Marchi}}$
Terrebonne	1.9
Barataria	1.2
Pontchartrain	2.5

The basin wide factor was used to guide the calibration of the partitioning coefficients. This calibration method assumes that all inlets within the same basin depart from the O'Brien-Jarrett-Marchi law prediction by the same factor, namely the basin wide factor. Each inlet conveys the flow for its effective tidal prism or "sub-basin," as described in the module development section under effective tidal prism. Within each basin there is a sub-basin assigned to every inlet link. The size of the sub-basin is determined by the partitioning coefficients, which distribute the total basin tidal prism to each of these inlets. The partitioning coefficients were adjusted until the ratio of the inlet area in the existing ICM-Hydro model dimensions matched the inlet area derived from the tidal prism calculation for each of the links within the same basin. For example, Figure 11 shows the sub-basin for link 349 within the Pontchartrain Basin. The inlet area from the ICM dimensions is 28,000 m^2. The initial partitioning coefficients produced an inlet area of 15,688 m^2 (calculated from the tidal prism using mean tidal range and the O'Brien-Jarrett-Marchi law), giving a sub-basin ratio of 1.8. Since this value is less than the basin wide factor of 2.5, the effective tidal prism was initially over-estimated. The partitioning coefficients were adjusted until the inlet area was 11,041 m^2, producing the ratio of 2.5. These calibrated partitioning coefficients are shown by the percentages in Figure 11.

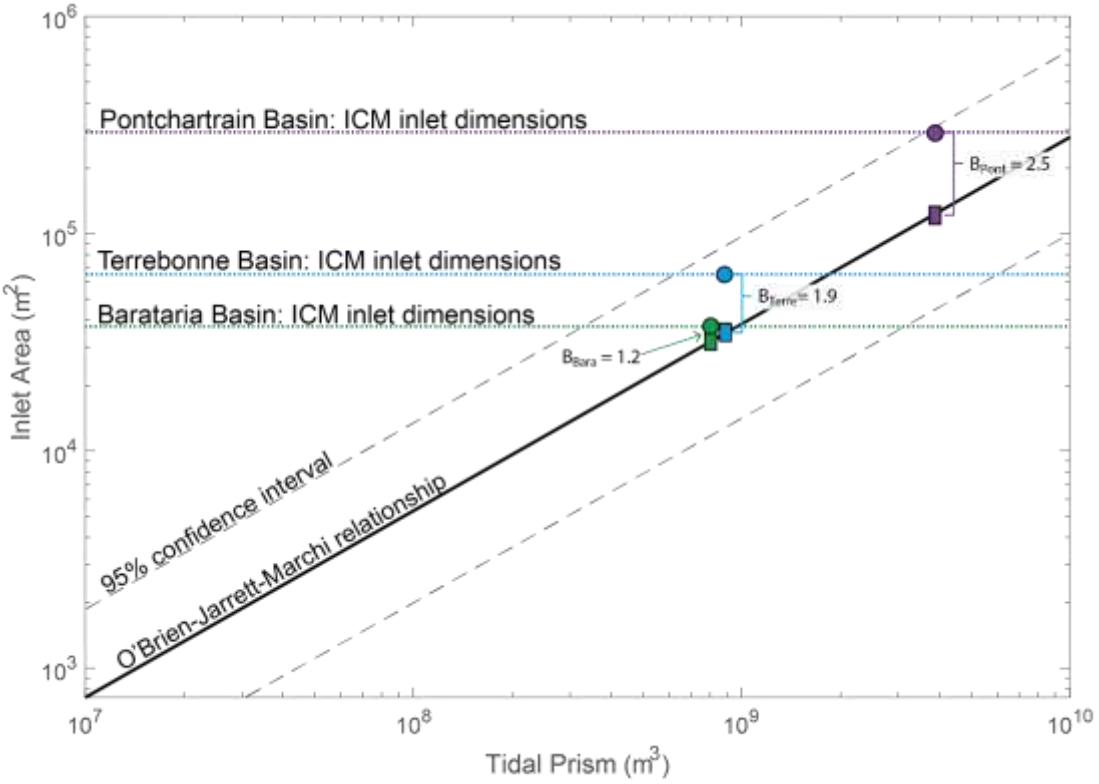

Figure 10. The O'Brien-Jarrett-Marchi relationship for the three basins calibrated. The horizontal dotted lines are the inlet areas from the ICM-Hydro inlet link dimensions. The inlet areas calculated from the ICM-Hydro tidal prisms (rectangles) are increased by the basin wide factor to match the ICM inlet dimensions (circles). All ICM inlet dimensions fall within the 95% confidence interval for the O'Brien-Jarrett-Marchi relationship.

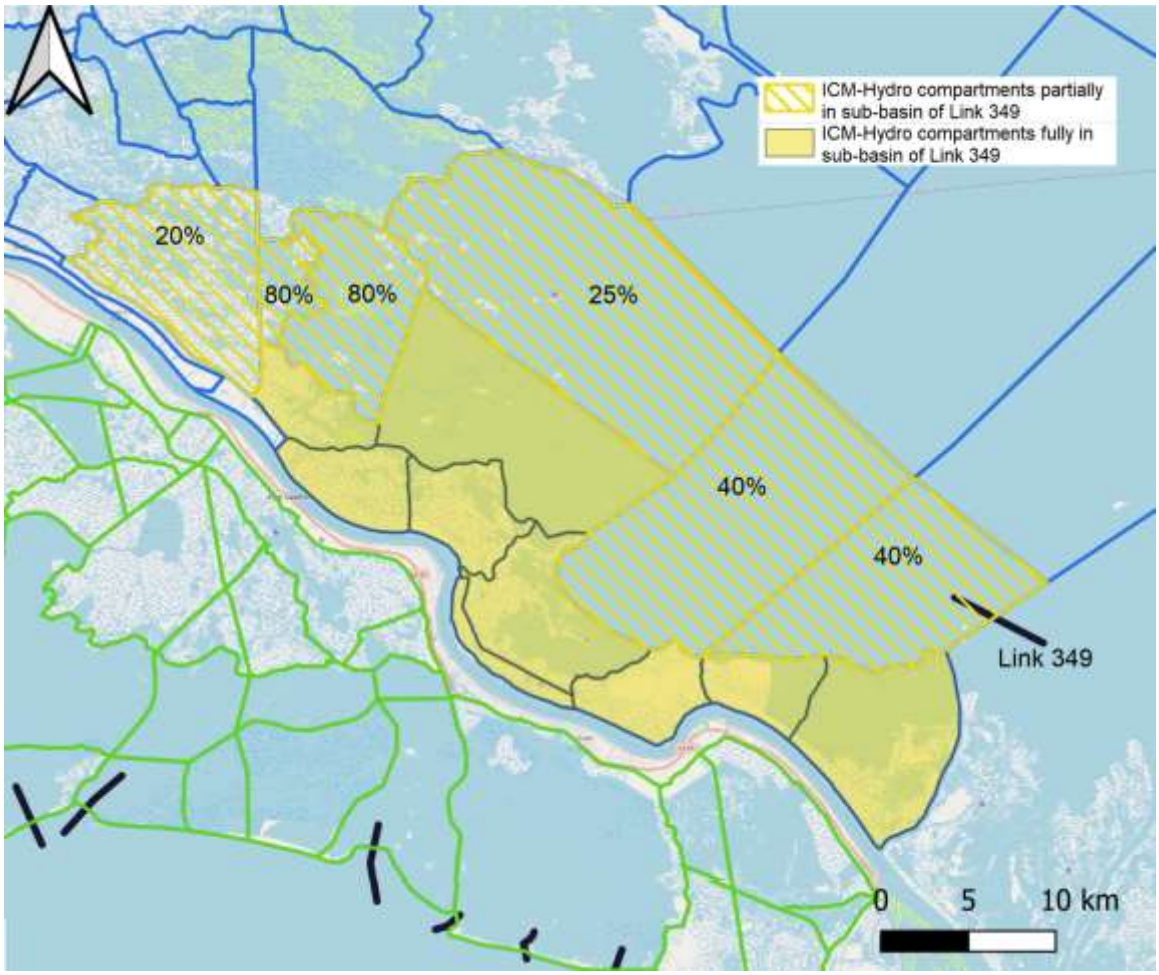

Figure 11. Sub-basin for inlet link 349. 100% of the tidal prism in the solid yellow ICM-Hydro compartments is a part of the effective tidal prism for inlet link 349. Yellow hatched ICM-Hydro compartments convey a portion of their tidal prism through inlet link 349, as indicated by the given percentages.

2.4 BARRIER ISLAND TIDAL INLET MODULE SCHEMATIZATION

This section describes steps of the BITI module that occur at each ICM timestep, including how the physical processes described above are incorporated.

Step 1: ICM-Hydro calculates and outputs the tidal prism for all ICM-Hydro compartments.

Step 2: Partitioning coefficients are applied to ICM-Hydro compartments to calculate the effective tidal prism for each inlet link.

Step 3: O'Brien–Jarrett–Marchi law is applied to each inlet link to estimate the cross-sectional area.

Step 4: Inlet aspect ratios are applied to convert cross-sectional area to width and depth.

Step 5: Inlet link attributes with updated dimensions are prepared for ICM-Hydro input.

3.0 BARRIER ISLAND DIGITAL ELEVATION MODEL (ICM-BI)

3.1 INTRODUCTION

One of the main objectives in updating the framework for the 2023 Coastal Master Plan is for the model to reflect the assumption that, for modeling purposes, the integrity of the Louisiana barrier islands will be maintained over time. Barrier island integrity will ultimately be defined by the Barrier Island System Management program (BISM). For the purposes of this modeling, integrity is assumed to include preventing and repairing barrier island breaches by maintaining a critical barrier island width, and by allowing for managed transgression of the islands. The assumption of barrier island integrity has been made to prevent storm-driven damage to the barrier islands—a stochastic process that cannot be predicted with certainty in space or time— from dominating the selection of specific coastal restoration projects for implementation. The second objective of updates for the 2023 Coastal Master Plan was to enhance the morphology evolution of ICM-BI by extending bathymetric evolution seaward at depths near the middle and lower shoreface in order to better reflect observed shoreface response.

3.2 MODEL DEVELOPMENT

The framework of BIMODE was modified in several ways to produce the ICM-BI workflow (Figure 12, Figure 13). First, the component of the model that predicted storm impacts to the barrier islands was removed. Although ultimately a process-based model framework that accounts for storm-driven effects to the barrier islands would enable predictions over a broader range of specific future scenarios, for the 2023 Coastal Master Plan these components are replaced with an empirical model of cross-shore island migration. An empirical model allows for a less scenario-specific or storm-specific prediction of future conditions and instead looks at past island migration to inform future conditions. Cross-shore migration rates for this component of the model, described below, are based on historic island (shoreface and shoreline) retreat rates and empirical model predictions of the variation in retreat rate under varying sea level rise (SLR) scenarios. This cross-shore retreat model evolves the shoreline and shoreface. Because the historic rates used to migrate the shoreline include the impacts of long-shore transport implicitly, the long-shore transport component of BIMODE is also removed. Secondly, an "auto-restoration" module is added that simulates placing sediment on (i.e., restoring) a barrier island if a critical threshold of minimum barrier island width is reached (Figure 13). These changes are made so the model is consistent with the assumption that barrier island integrity will be maintained by the

BISM program over the simulation period. Third, post-processing code was added to interpolate the model output to a fixed grid domain, which facilitates incorporation of results into the ICM-Morph domain. Lastly, the model was updated to allow marsh islands and interior marsh (i.e., marsh that falls within the ICM-BI domain but is not part of a barrier island) to keep pace with relative sea level rise (RSLR). These changes are described in more detail below.

The elements of BIMODE responsible for implementing vertical relative elevation change due to SLR and land subsidence are retained. Also retained are the elements responsible for predictions of bayside shoreline erosion (horizontal marsh edge retreat) based on values derived from observations, as well as the method by which shorelines are identified each year. The Mean High Water (MHW) level from nearby compartments in ICM-Hydro is passed to ICM-BI each year and used to identify shorelines within ICM-BI, defined as the intersection of that MHW level with the elevation profile for each cross-shore transect.

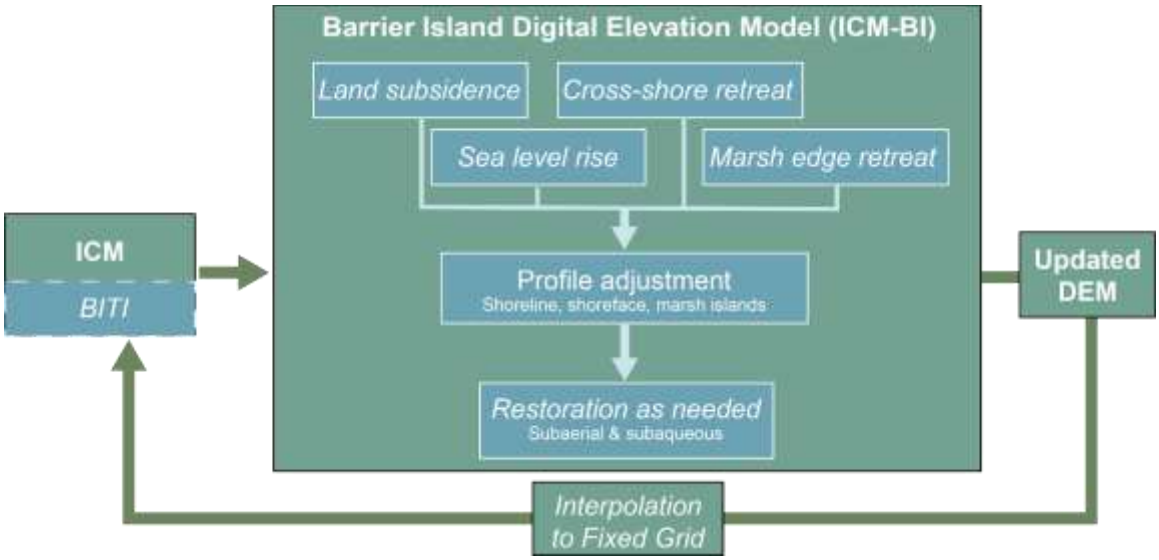

Figure 12. Flow diagram of ICM-BI and BITI.

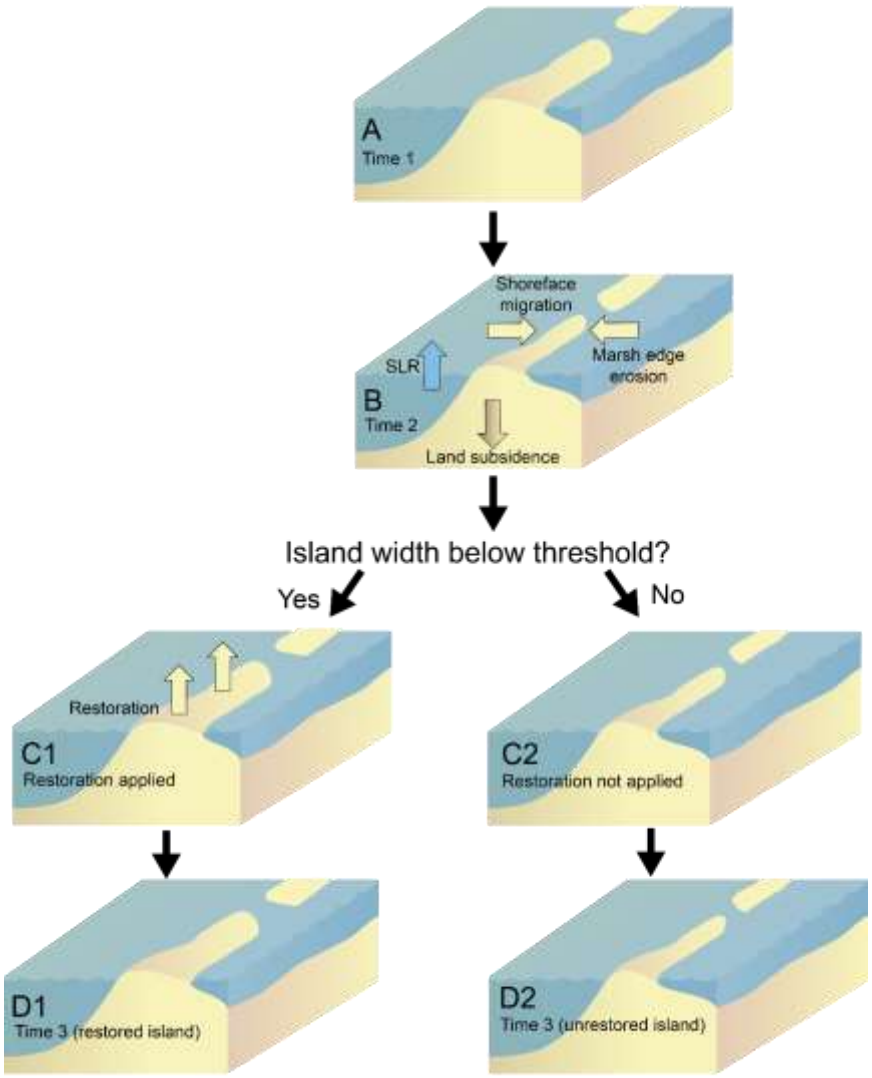

Figure 13. Conceptual diagram of modeled barrier island evolution. (A) Digital Elevation Model (DEM) for a section of the coast with two barrier islands and an inlet. (B) SLR and land subsidence vertically adjust the profiles; spatially varying cross-shore retreat rates are used to migrate the shoreline and the upper and lower shoreface; and marsh edge erosion rates are used to migrate the bay shoreline. A restoration template is then applied (C1) or not (C2) to a restoration unit (island or portion of the island) depending on if that unit has fallen below a prescribed threshold. (D1) and (D2) final DEM with or without restoration after the model timestep. Base diagram modified from symbols acquired from the Integration and Application Network, University of Maryland Center for Environmental Science (ian.umces.edu/symbols/).

CROSS-SHORE MIGRATION RATES

ICM-BI includes six regions (Figure 14–Figure 16), each consisting of a variable number of cross-shore profiles (Barataria, 296 transects; Caminada, 535 transects; Terrebonne, 190 transects; Isles Dernieres, 450 transects; Breton, 269 transects; Chandeleurs, 640 transects) that run approximately perpendicular to the shoreline of the barrier islands (Figure 19).

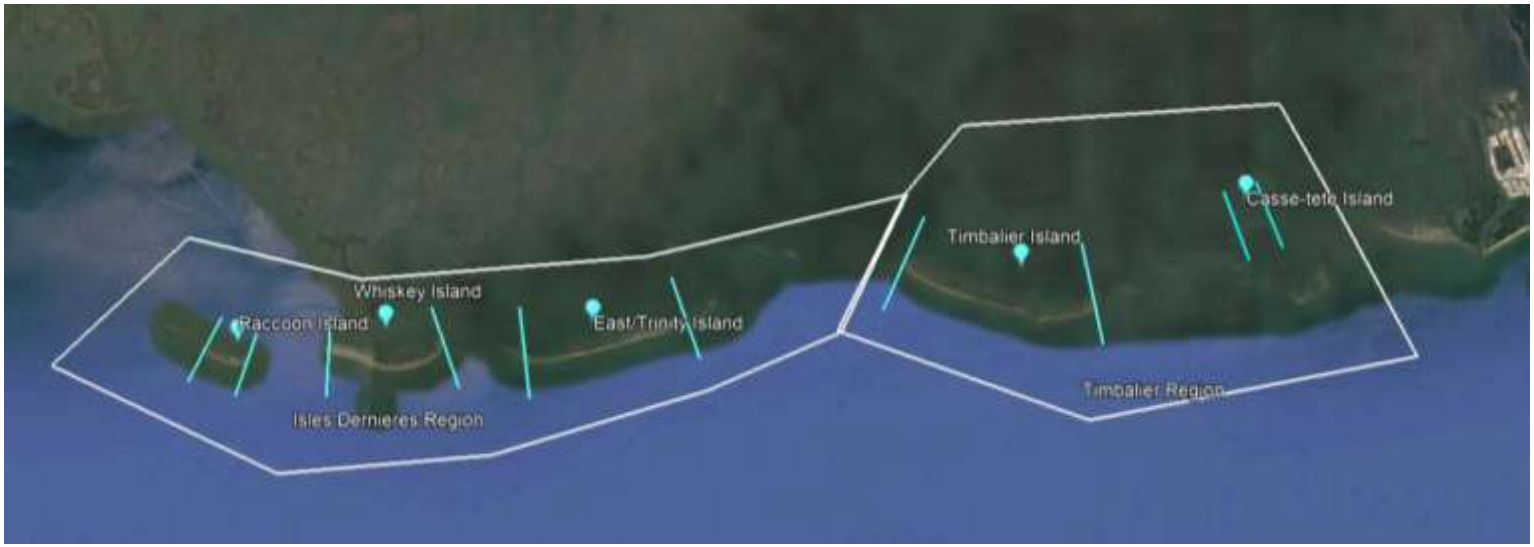

Figure 14. Restoration units for the Isles Dernieres and Timbalier regions. Regions are shown in white (Isles Dernieres region to the west, Timbalier region to the east), restoration unit delineations shown in blue. The Casse-tete Island and Raccoon Island restoration units were delineated during model development, but auto-restoration was not applied to these units (see Appendix 1).

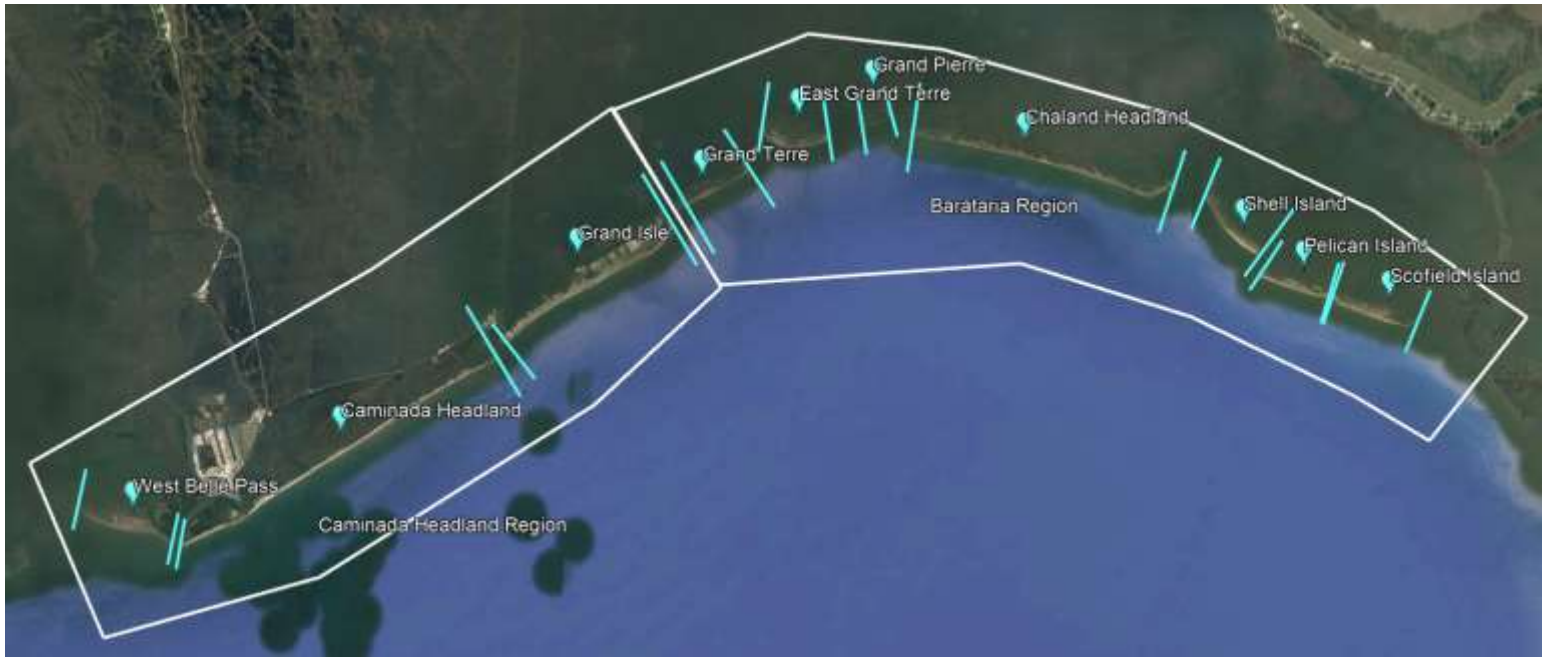

Figure 15. Restoration units for the Caminada Headland and Barataria regions. Regions are shown in white (Caminada Headland region to the west, Barataria region to the east), restoration unit delineations shown in blue. Auto-restoration is not applied to the Grand Isle unit for the 2023 Coastal Master Plan. (see Appendix 1).

Figure 16. Restoration units for the Chandeleurs and Breton regions. Regions are shown in white (Chandeleurs Region to the north, Breton Region to the south), restoration unit delineations shown in blue.

The cross-shore resolution of points within each profile is 5 m with a long-shore spacing between profiles of approximately 100 m. Cross-shore migration rates vary for each cross-shore profile (Figure 17). The new cross-shore position of each depth segment for each profile is determined using the following relationship:

$$x_{new} = x_{old} + \left(\frac{dx}{dt}\right) * dt \qquad (7)$$

where x_{old} is the old position of the depth; x_{new} is the new depth position; dx/dt is the cross-shore migration rate; and dt is the timestep. The term dx/dt is calculated based on historical rates (dx/dt) modulated by a term to account for the potential influence of relative SLR on cross-shore retreat:

$$\frac{dx}{dt} = \alpha \left(\frac{dx}{dt}\right)_H \qquad (8)$$

where α is a modulation term of the historic retreat rates derived from analysis of the impact of SLR on dx/dt.

Isobath migration rates developed by Beasley et al. (2018, 2019) were initially used within the model. Because these data do not extend to the Breton and Chandeleur regions, the same methodology was followed to derive historic retreat rates for these regions using Barrier Island Comprehensive Monitoring Program (BICM) data. Historical data from the earliest time period available were used in calculating these rates. The individual surfaces used were compiled from surveys taken over several years (for example, the Chandeleur surveys were taken in 2006 and 2007), therefore each data set is referred to by the decade of acquisition. Retreat rates for the Central Coast and Chandeleur regions were initially calculated over the period of 1880s to 2010s and 1920s to 2000s, respectively.

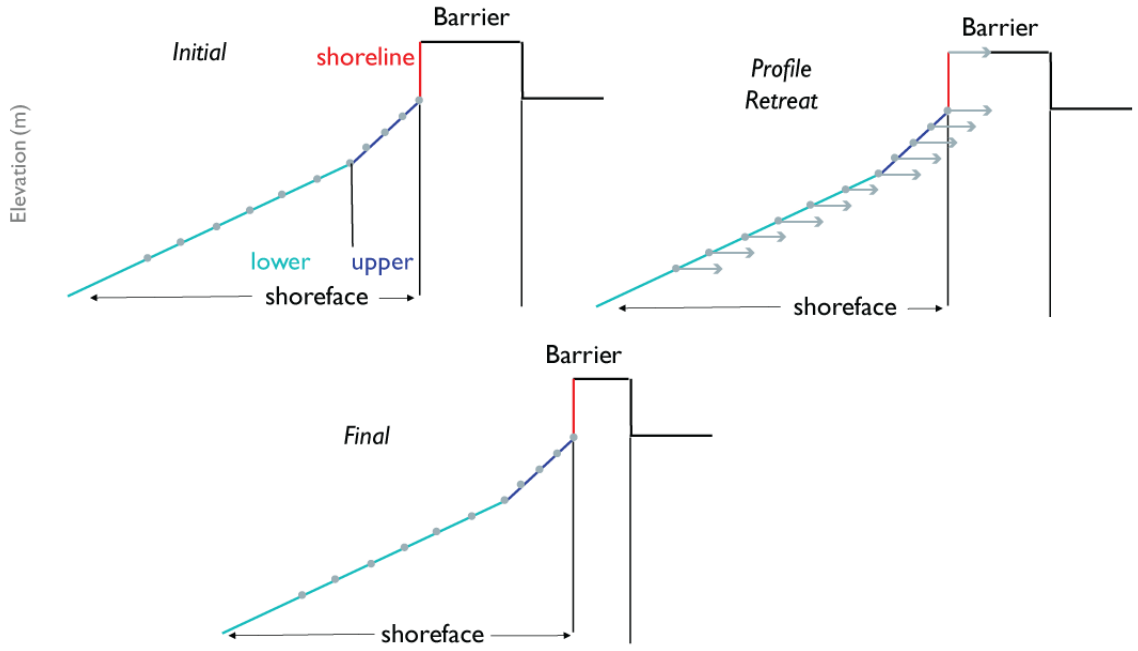

Figure 17. Conceptual diagram of cross-shore island and shoreface retreat. Each depth along the profile retreats at a specified rate (dx/dt in Eq. 7). Historical shoreline retreat rates are used to update the morphology of the subaerial island, resulting in realistic barrier island narrowing.

Sensitivity testing was done during the development of ICM-BI to refine the degree to which long-shore and cross-shore variability in the cross-shore retreat rate should be included, as well as the time period over which to perform the calculation. Cross-shore retreat rates were calculated for each profile and cross-shore depth ranging from the shoreline to 12 m water depth. During initial testing, a rate was calculated and applied to each isobath on every profile within the ICM-BI domain without smoothing.

There were two issues using these depth-variable cross-shore retreat rates. First, the calculated shoreface retreat exhibited considerable long-shore and cross-shore variability, which is the result of the combined influence of short- and long-term processes. Variability in the upper shoreface and surf zone is particularly high, likely as a result of this highly dynamic portion of the coast being dominated by processes occurring over short timescales and relatively small spatial areas (sand bar migration, post-storm shoreline retreat and recovery, etc.). Throughout the profile, however, variability in shoreface retreat rate and slope occurs due to, for example, decadal-scale oscillations in storm frequency and intensity (Beasley et al., 2019).

Second, these rates introduced unrealistic behavior to the shoreface in some locations, including deeper points within a profile overtaking shallower points. This behavior is the result of the calculated retreat rates including the migration of relatively dynamic features such as offshore shoals. A shoal may be present within a profile in the initial Digital Elevation Model (DEM) and then migrate in the alongshore direction and out of the profile by the time of the next DEM, leading to an artificially high retreat rate that does not reflect the migration of the underlying shoreface, or vice versa (Figure 18, Top). For example, when the transect profile crossed an isobath twice, as in the case of a profile with an offshore shoal, the offshore crossing was used in the retreat calculation. Long-shore averaging was explored as a way to mitigate this issue but was found to be ineffective due to high long-shore variability within the retreat rate profiles. In particular, the spatial mean produced an unrealistic cross-shore retreat rate profile in areas with sharp long-shore gradients in shoreface behavior.

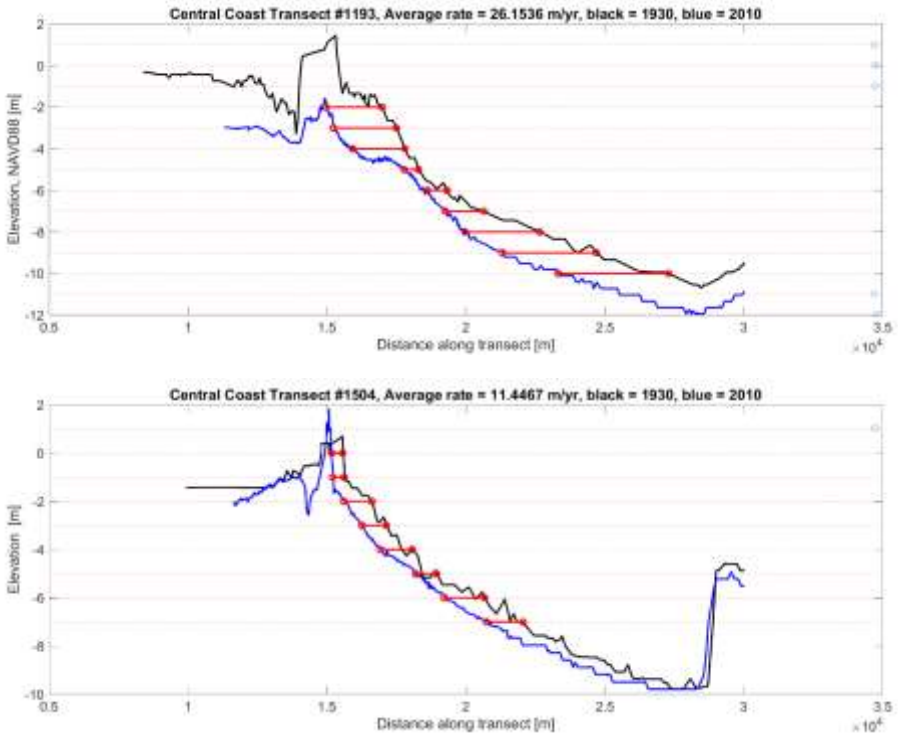

Figure 18. Top: Example calculation of cross-shore retreat rates for a profile demonstrating variability along the shoreface profile. An inflection is present around the 4–6 m contour in the 2010s profile that was not present in the 1930s and likely appears due to ebb tidal delta lateral expansion. This feature leads to low calculation retreat rates for the 5 m and 6 m contours that do not reflect the migration of the lower shoreface. Bottom: Calculation of cross-shore retreat rates for a profile. Manual quality control is used during isobath cross selection to ensure the points reflect the migration of the shoreface and not more ephemeral, smaller-scale features. Note that this profile extends to Ship Shoal (the abrupt bathymetric high at the end of the profile).

As an alternative to averaging, the team identified index profiles (Figure 19) along the coast that are representative of the cross-shore retreat for a given sector of coast. The location of each index profile was chosen to represent the dominant morphological characteristics of an area. These profiles were selected based on the geomorphodynamics of the coast that result in long-shore variability in shoreface and near-shore behavior, spanning various geomorphic environments and based on interpretation of seafloor and shoreline change data dating back to the 1890s (e.g., Penland et al., 1988; List et al., 1994; Miner et al., 2009a, b; Applied Coastal Inc., 2020). The cross-shore retreat rate for each index profile was then interpolated in the alongshore direction to produce retreat rates for every profile within the domain. In the initial testing of the cross-shore retreat methodology that utilized automated extraction procedures, similar issues in the retreat rates were identified related to dynamic features such as ebb deltas along the profile. This issue was addressed by careful manual quality control of the isobath-profile crossing points, with crossings selected such that the calculated rate would reflect average movement of the shoreface (Figure 18, Bottom). Three variations on this approach were considered: (1) cross-shore retreat rates varying with depth with a single mean value calculated for the upper shoreface and a second mean value calculated for the lower shoreface; (2) a single mean cross-shore retreat rate for each profile with no variation with depth; and (3) a single mean cross-shore retreat rate for each profile calculated from the upper shoreface rates (shallower than 7 m) with no variation with depth. Retreat rates were calculated over the period of 1930s to 2010s (Central Coast) and 1920s to 2000s (Chandeleurs), and the different methods were assessed by hindcasting over the period of 1980s to 2010s along the Central Coast and over the period of 1920s to 2000s along the Chandeleurs.

Varying the cross-shore retreat rate with depth (approach 1) was found to introduce depth-varying bias in the predicted profile, where the retreat for the upper or lower shoreface of some profiles was over- or under-predicted. Similarly, using the mean retreat rate of the entire profile (approach 2) led to an over-prediction in the retreat of the upper shoreface. This bias was found to be a result of variation in the shoreface retreat and slope over time. The retreat rate of the upper and lower shoreface varies with oscillations in storm frequency and intensity, with the lower shoreface behaving differently than the upper shoreface, (Beasley et al., 2019). This introduces the potential for systematic bias with depth when applied over decadal scales. For example, the lower shoreface will migrate faster during periods of intense storminess compared to the long-term average, so applying the long-term average in the model to predict an intense storminess period will result in a predicted profile that is biased offshore throughout the lower shoreface. Because variability in storminess over the 2023 Coastal Master Plan modeling period cannot be predicted, a single value of cross-shore retreat rate was applied for each long-shore profile in the model. This approach was found to minimize the introduction of systematic bias with depth. The value calculated for the upper shoreface (shallower than 7 m) was used (approach 3) so the model had the highest accuracy of prediction (compared to observations) for the subaerial portions of the island, shoreline position, and upper shoreface.

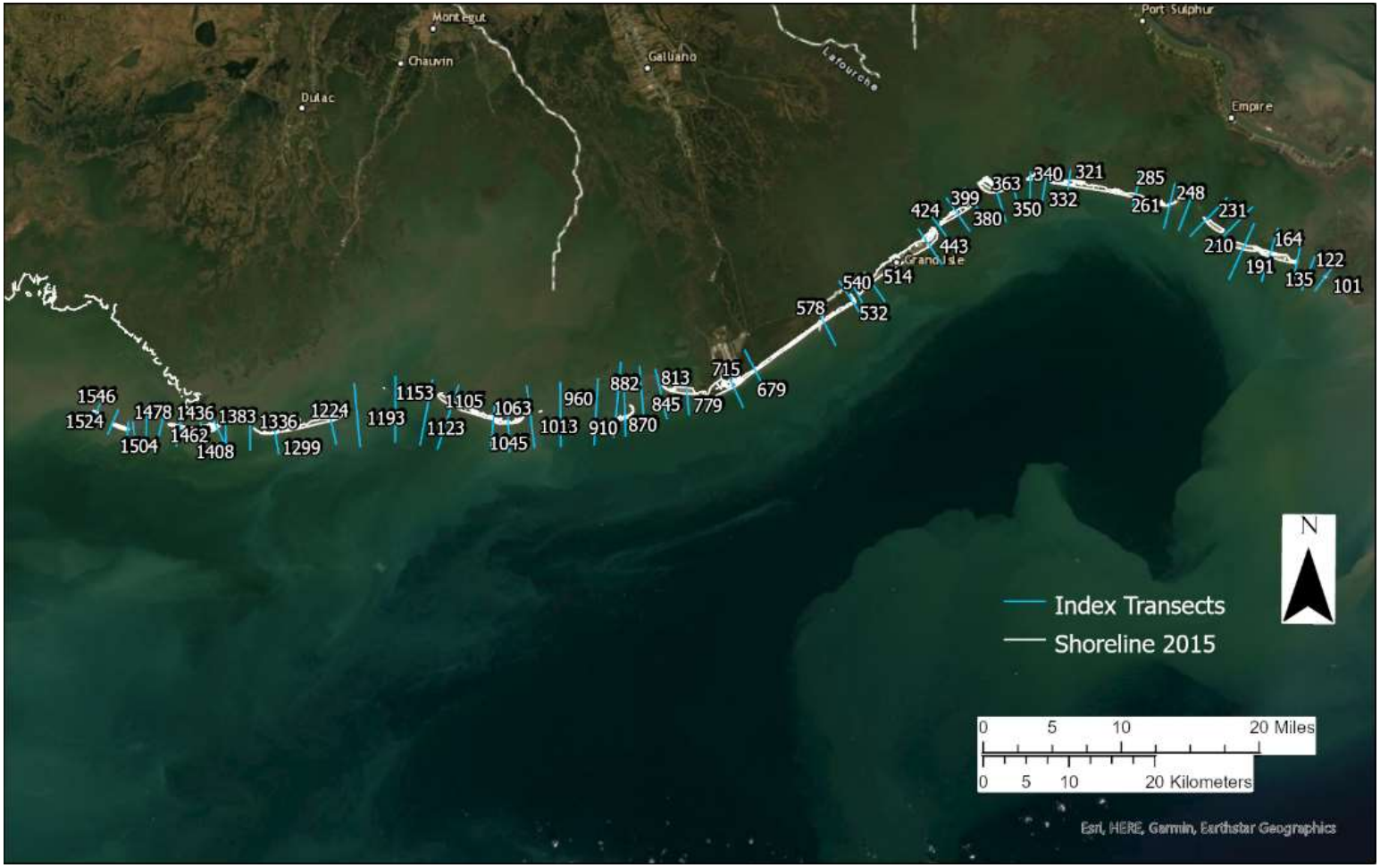

Figure 19. Index profiles used to calculate the cross-shore retreat rate.

There were several regions of the coast where the cross-shore retreat rates were modified to reflect ongoing and future anthropogenic influences that would not be captured in the historic rates. Coastal protection structures (e.g., breakwaters, sea walls) have been constructed at Raccoon Island and Grand Isle; in order to reflect the influence of these measures, the cross-shore retreat rate of the shoreline and uppermost shoreface (<3 m) are set to zero. However, lower shoreface rates for these sections of hardened coast were allowed to evolve based on the historical retreat rate to simulate shoreface steepening as observed in Louisiana in the presence of shoreline armoring. Cross-shore retreat rates for the entire shoreface were additionally set to zero for profiles intersecting Belle Pass Channel in order to capture the likely response of this area given the jetties at this location.

Cross-shore retreat rates under scenarios of SLR higher than historical rates in Louisiana were calculated using the Barrier Island and Inlet Environment (BRIE) model, which explicitly accounts for trends in shoreface and shoreline retreat as a function of RSLR (Nienhuis & Lorenzo-Trueba, 2019). This model was used to ensure that predicted migration rates are realistic and consistent with future rates of RSLR. The model was first parameterized using values representative of the Louisiana coast and was used to predict shoreface retreat rates under historical RSLR. These rates were compared to those calculated from Beasley et al. (2019) and Beasley (2018) to verify that model predicted rates (~5–6 m/yr averaged across isobaths) were consistent with observed shoreline and shoreface behavior (retreat rates vary between 2–36 m/yr over the entire coast with a median retreat of ~12 m/yr).

For the ICM-BI SLR sensitivity simulation, shoreface and shoreline retreat rates were modeled using a shoreface depth of 14 m, a median grain diameter of 160 μm, and a range of RSLR rates from 5 to 17 mm/yr. The model results were then normalized using historical RSLR rates (5 mm/yr in the Chandeleurs and Breton regions and 9 mm/yr in the Central Coast regions) to derive a linear regression model for calculating the modulation term (α in equation 8) as a function of the future RSLR rate (Figure 20). The parameters of the fit of this line (slope, intercept) are used within ICM-BI to calculate the retreat rate modulation term from the eustatic sea level rise and subsidence rates for a given ICM scenario. Because the shoreline and shoreface modulation terms were similar, one regression model was selected representing the average of the two.

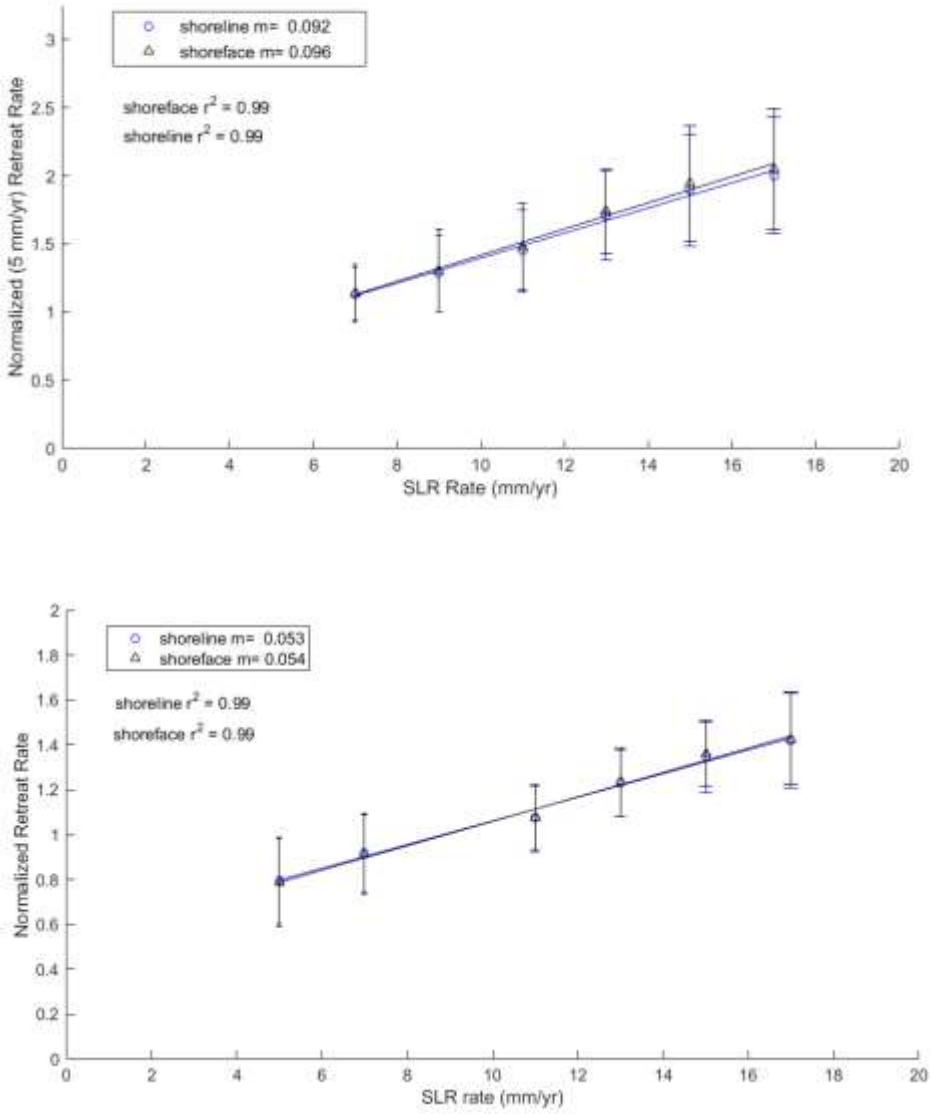

Figure 20. Shoreline and shoreface retreat rates modeled by BRIE for different RSLR rates. Top: Retreat rates are normalized by a RSLR rate of 5 mm/yr to represent the additional retreat caused by higher rates of RSLR. Bottom: Retreat rates are normalized by 9 mm/yr to represent the additional retreat caused by higher rates of RSLR. The BRIE model predicts a time-varying retreat rate; values show are the mean (circle, triangle) and standard deviation (whisker) over the model run for each RSLR rate. The best fit lines to the shoreline and shoreface results are fit through the mean values and are used to calculate the modulation term for future rates of RSLR in ICM-BI.

BAYSIDE SHORELINE EROSION RATES

Bayside erosion rates were determined from the marsh edge erosion rate raster provided to the Coastal Protection and Restoration Authority (CPRA) by USGS. Only values along the bayside barrier island shoreline were extracted from the provided USGS raster. The bayside barrier island shoreline was created using the 2015 BICM shoreline (Applied Coastal Engineering, Inc. & CDM Smith, 2018) which was updated to include a recent coastal restoration project on Shell Island East (Lanaux Island) using 2019 aerial imagery from Google Earth. The bayside erosion rates were extracted from the raster at the points where the ICM-BI transects intersect the shoreline. In cases where multiple marsh edge erosion rates exist on a transect, the median value was used. Bayside erosion rates along the Caminada Headland were set to 0 m/yr to reflect the placement of breakwaters along the bayside shoreline.

ASSUMPTION OF BARRIER ISLAND INTEGRITY: ISLAND RESTORATION IN THE FRAMEWORK

A key assumption considered in the development of ICM-BI for the 2023 Coastal Master Plan is that BISM will maintain the integrity of the barrier islands even as coastal processes and SLR result in cross-shore migration (i.e., managed transgression). To capture this assumption, ICM-BI implements auto-restoration within the model, where all profiles that fall within a "restoration unit" (island, headland, or segment therein) are restored using a restoration template if the width of the unit falls below a defined critical threshold.

Barrier islands, headlands, and/or groups of adjacent cross-shore profiles that comprise shoreline segments are grouped together in the model to form "restoration units", which are used in implementation of auto-restoration in the model (Figure 14–Figure 16). If 10% of profiles that form the restoration unit fall cross a critical threshold, the appropriate restoration template is applied to the entire unit (a template varies according to the restoration unit and its morphological type: barrier island or headland). This percentage is set at 10% of the profiles within a restoration unit so that restoration is not triggered by a small number of profiles crossing the threshold. The 10% of profiles triggering restoration do not need to be contiguous within the restoration unit. The critical threshold for a barrier island profile is set at the subaerial width of the island falling below 75% of the full subaerial width of the restoration template associated with that island. The width of a barrier island is defined as the distance from the bay shoreline to the Gulf shoreline, with the island itself automatically identified within the model as the "Gulfward most contiguous land mass" in each profile. The threshold for headlands is defined as the shoreline eroding past a critical point. The Port Fourchon area of the Caminada Headland that is fronted by segmented breakwaters is assumed to "hold the line." For this "hold the line" area of Port Fourchon, the critical point is the shoreline eroding past the location of the rear dune toe. The rear dune toe is defined as the intersection of the dune with the back-barrier marsh or backbarrier flat, where the slope transitions from the steep rear face of the dune to a relatively flat slope. For the rest of the Caminada and Chaland Headlands, the critical point

is set as the shoreline eroding past the location of the dune crest in the initial condition DEM (i.e. the elevation of points within the domain at the start of the simulation, referred to as “existing conditions” in the 2023 Coastal Master Plan). When auto-restoration occurs, all profiles are restored to the elevation of the restoration template, therefore less elevation (~less sand) will be added to those profiles within the unit that have not crossed the critical threshold.

The auto-restoration template applied within the model varies spatially to be consistent with previous and/or expected restoration action for each restoration unit. The restoration templates used for each unit are provided along with their source in Appendix A, with an example template shown in Figure 21.

When triggered, the auto-restoration template is applied unilaterally across a restoration unit at one timestep (one year). For each barrier island profile, the auto-restoration template is first aligned to the residual island profile within the model so that the peak in elevation in the template corresponds to the cross-shore location of the peak elevation in the model profile (Figure 22). For each headland profile, the peak in the restoration template is placed at a specified distance relative to the location of the dune crest for the most recent prior restoration (Figure 23). For the “hold the line” area of Port Fourchon defined above, the setback distance of the restoration is set to 0 m and the restoration template is always placed at the same location once the prior template erodes past the dune crest. For the remainder of Caminada Headland and the Chaland Headland the setback distance depends on the width of the restoration template for each unit. In these areas, the dune crest of the restoration template is placed at the location of the former rear dune toe after the shoreline erodes past this location, thereby allowing the headland to retreat landward. In all cases, the elevation of any cross-shore location that is lower than the template elevation is then raised to the elevation of the restoration template. The restoration templates are adjusted to add the MHW level for that timestep in the model so that the restoration template elevations keep pace with SLR.

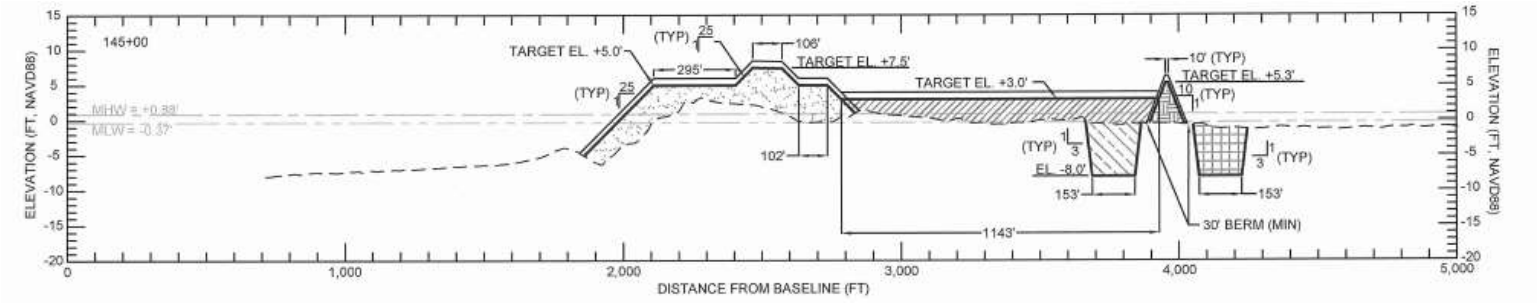

Figure 21. Example of a barrier headland restoration template for the Terrebonne restoration project TE-143 (from CEC, 2019).

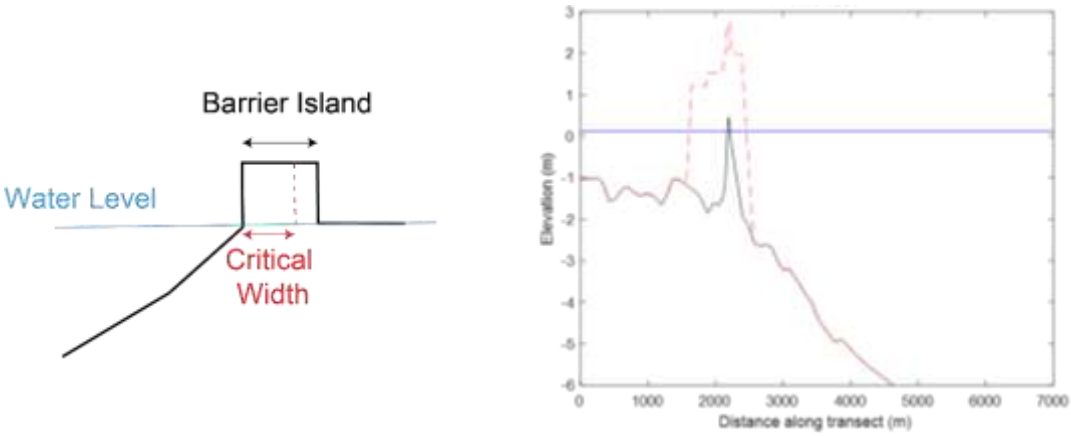

Figure 22. Implementation of auto-restoration of a barrier island within the ICM-BI model. If the subaerial width of at least 10% of profiles within a restoration unit fall below the critical width (left), the restoration template is applied to all profiles within the restoration unit. For example, the subaerial width of the island in the profile on the right has fallen below the critical threshold after application of cross-shore retreat and subsidence (pre-restoration profile in black, water level shown as horizontal blue line). The barrier island restoration template is therefore applied (red dashed line), aligned so that the peak of the restored profile is above the peak of the existing island.

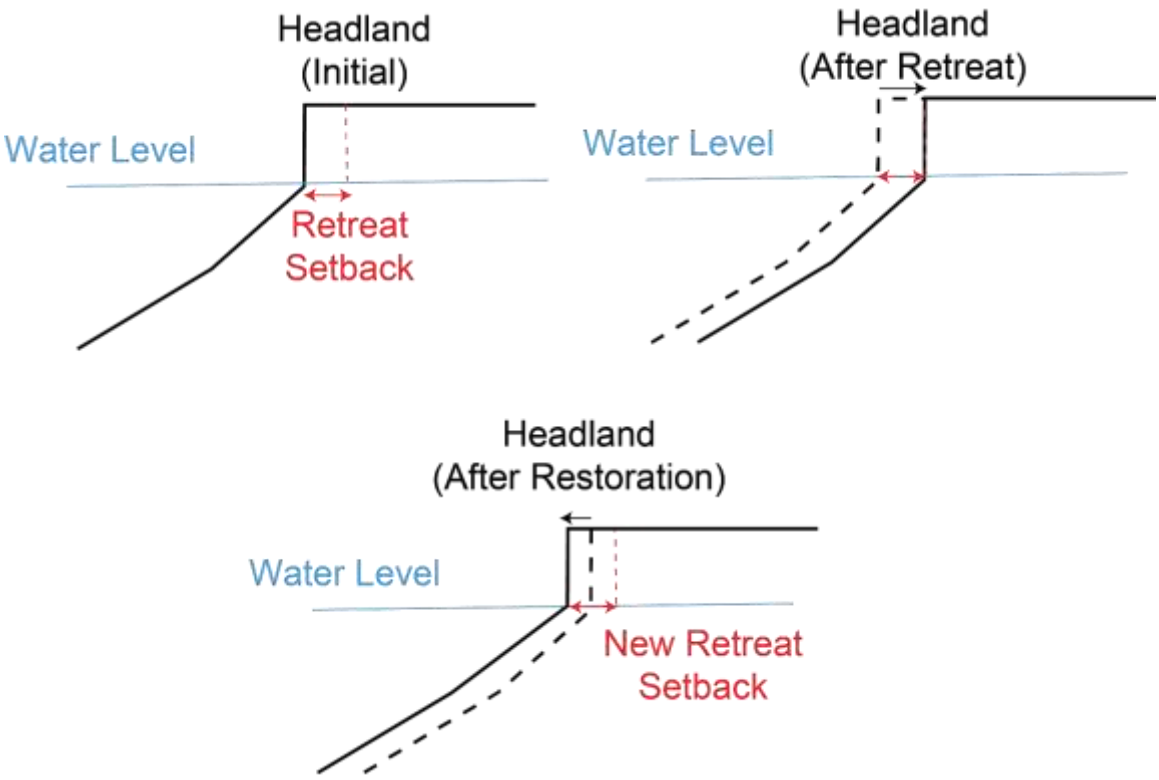

Figure 23. Implementation of auto-restoration of a headland within ICM-BI. Each profile has a prescribed retreat setback. If the shoreline of at least 10% of profiles within a restoration unit cross the retreat setback, the restoration template is applied to all profiles within the restoration unit. The retreat setback is then reset based on the restored profile.

Per technical recommendations of the Predictive Model Technical Advisory Committee (PM-TAC) and model decision team (MDT), other methods of applying the restoration template were considered: 1) Raising the height of each profile over multiple timesteps, simulating the elevation of all profiles within the unit being raised gradually over multiple years until they reached their full template height; and 2) Splitting restoration units into subsets of profiles that are restored over multiple years, simulating restoration occurring spatially over time within a restoration unit (e.g., moving alongshore from east to west). The first alternate approach was not implemented because it does not reflect the reality of how Louisiana barrier islands are restored. The second alternate approach was not implemented for several reasons. The first of which is that sand placement for most restoration units would occur over a time scale closer to one year than two years. Secondly, cross-shore retreat between two phases of restoration could potentially introduce discontinuities between adjacent profiles within a unit, if restoration in the model does not occur simultaneously. Lastly, the alongshore extent of the restoration units themselves can be modified (shortened) to practically achieve the same result of

limiting the alongshore extent over which restoration is applied in a single timestep of one year.

Note that the auto-restoration methodology developed here provides a framework for explicit testing of the resilience of various templates of barrier islands during future master plan iterations if process-based methods for evaluating cross-shore retreat and explicit storm impacts are included in future model developments. In addition, it would enable estimates of the sediment volumes needed to maintain barrier island integrity to be derived.

MODEL DOMAIN AND ELEVATION CHANGE OF BASIN MARSH

For the 2023 Coastal Master Plan, a modification was made in the way ICM-BI passes information to the rest of the ICM. The 2017 BIMODE grid configuration consisted of a set of profiles with fixed orientation relative to the coast (nominally perpendicular to the shoreline, although curvature in some areas causes slight deviations). Each elevation point along the profile was referenced as a distance relative to the origin point of the profile. This convention allows the model grid to migrate with the barrier island landforms; as the islands and shoreface move, the model points themselves also change location. ICM-BI retains the migrating grid for internal calculations. Integration of ICM-BI with the rest of ICM-Morph, however, required ICM-BI to output to a fixed set of grid points. To address this need, a set of grid points was extracted from the initial distribution of ICM-BI grid points at the beginning of the model run. The output of ICM-BI was interpolated to this set of grid points after each year using linear triangulation. Transect points for interpolation at the edges of regions were migrated toward the center of the region by 10 m to ensure there were zero “no data values” output by the interpolation. The extent of the fixed grid was set using the distance the islands would migrate under a high SLR scenario so that islands would not migrate out of the fixed grid.

Because of the need to extend the profiles inshore to accommodate barrier island migration, the fixed grid includes some interior marsh islands and headland marsh within the ICM-BI domain. Areas identified as marsh would be expected to keep pace with RSLR through processes of marsh accretion. To prevent unrealistic submergence in the model because the process of marsh accretion is not captured in ICM-BI, subaerial elevation points within the back basins of the ICM-BI domain are compared to marsh delineation criteria used in ICM-Morph (i.e., the “blue line curve”; Baustian et al., 2020). This relationship sets the annual mean inundation depth threshold between water and marsh as a function of salinity; those elevations that are above this threshold are identified as “marsh” in ICM-BI. Annual salinity values in year 1 and 50 of the G031 ICM test run were examined in the ICM-Hydro compartments containing barrier islands. A threshold mean annual depth of 17 cm was selected, which covers a salinity range of 20.9 ppt to 24.5 ppt. Because the DEM and thus marsh elevations are in NAVD88 and ICM-Hydro communicates a MHW value each year to ICM-BI, ICM-Hydro values of MHW are converted to mean sea level (MSL) using a datum conversion tool, so they can be referenced to the mean annual inundation depth of 17 cm. Areas delineated as marsh then keep pace with RSLR, retaining their elevation relative to MHW as the model runs (i.e., elevation is added to

offset the impacts of subsidence and eustatic sea level rise). A similar approach is used at headlands, with the same process applied to raise the elevation of marsh that is leeward of the headland auto-restoration area. The boundary between barrier island and headland auto-restoration areas and "interior" marsh, where the accretion formulation is used to help marshes keep pace with RSLR, is prescribed for the first model timestep based on manual delineation. As auto-restoration occurs, the leeward edge of each island is updated to be the bayside edge of the auto-restoration template.

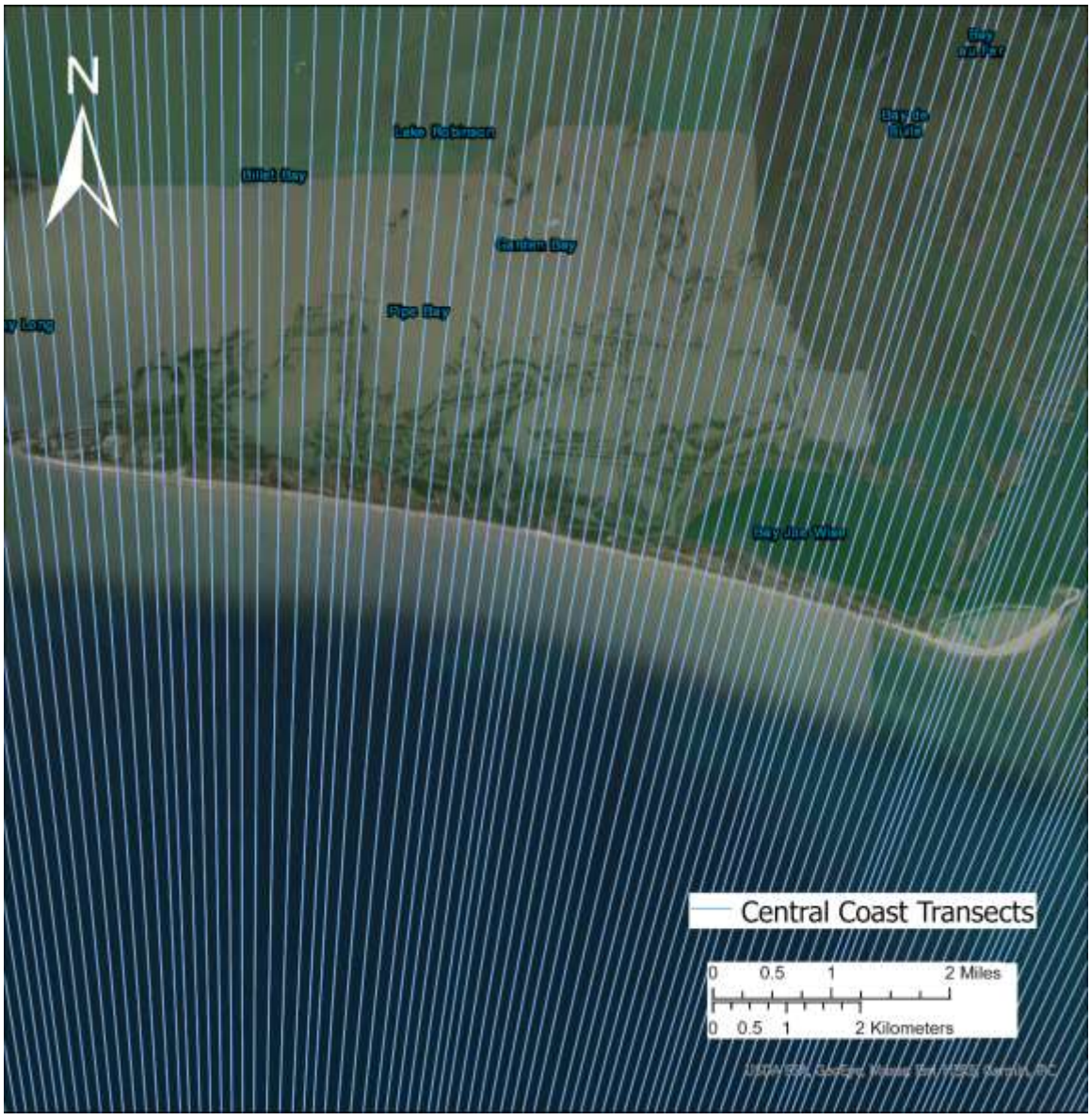

Figure 24. An example of the transects along Chaland Headland that make up the ICM-BI model grid.

A similar approach was used to address geomorphic change at Grand Isle. Because it is developed, with hurricane protection features managed by the U.S. Army Corps of Engineers, Grand Isle will not be managed under the BISM program, and auto-restoration based on fixed thresholds of barrier integrity loss would not accurately capture management of the island. However, coastal protection measures are expected to be used to maintain its subaerial elevation relative to MSL. As a result, Grand Isle is prescribed to keep pace with RSLR using the same approach that is used for interior marsh areas.

SENSITIVITY TESTING: PROCESSES TRIGGERING BARRIER ISLAND AUTO RESTORATION

To determine if RSLR would significantly impact restoration unit auto-restoration frequency, a sensitivity test was conducted for a coastal reach with two restoration units: Caminada Headland (a headland restoration unit) and West Grand Terre (a barrier island restoration unit). Five simulations were conducted to evaluate the contribution of different model processes to triggering auto-restoration: (1) cross-shore retreat only; (2) cross-shore retreat and subsidence; (3) cross-shore retreat, subsidence, and SLR (4) cross-shore retreat and bayside retreat; and (5) all processes activated (cross-shore retreat, bayside retreat, subsidence, and SLR). In all cases, auto-restoration was triggered with the previously described thresholds. The model was initialized with a combination of datasets that included the following: for the central, a 2010s DEM (Applied Coastal Science and Engineering, 2020) that covered the shoreface and near-shore regions, supplemented with a draft version of the NGOM2 DEM for the subareal parts of the coast and part of the back-barrier. For the Chandeleur Islands, we used the USGS BICM2 DEM (Stalk et al., 2017). Following initialization, the model was run for a 50-year period.

Results of the sensitivity testing indicated that, as expected, auto-restoration of the barrier island unit is triggered earliest when all the erosional processes of the model are included in the simulation; this early restoration action and subsequent loss of the restored subaerial volume resulted in triggering auto-restoration during years 11 and 47 of the model (Figure 25). Subsidence and SLR are dominant factors compared to bayside retreat, with auto-restoration triggered only 2–3 years later in simulations including these processes when compared to the simulation including all processes. We note that these processes reduce the width of the island via submergence of both the Gulf and bay shorelines. Auto-restoration in the simulations that only account for cross-shore retreat of the Gulf shoreface occurred 10 years and 17 years later, respectively, compared to simulations including all processes. The overall volume of placed sediment during the first auto-restoration was reasonably consistent between all simulations.

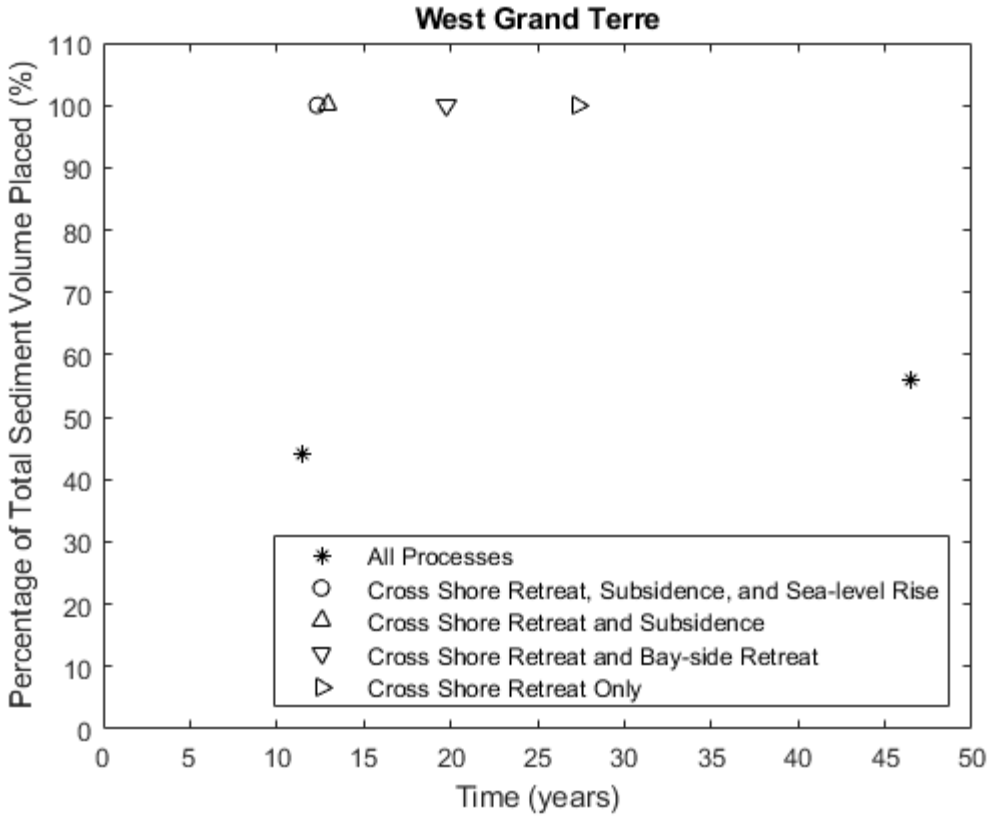

Figure 25. Restoration frequency for West Grand Terre for model simulations including different combinations of processes, including: (1) cross-shore retreat only; (2) cross-shore retreat and bayside retreat; (3) cross-shore retreat and subsidence; (4) cross-shore retreat, subsidence, and SLR; and (5) all processes activated. Sediment volumes are normalized by the total sediment volume placed.

The frequency of auto-restoration at Caminada Headland was insensitive to the inclusion of different processes governing profile subaerial width reflecting that cross-shore retreat dominates at this location. The required restoration volume increased with the inclusion of subsidence and SLR, reflecting the additional sediment needed to maintain a subaerial profile given these processes.

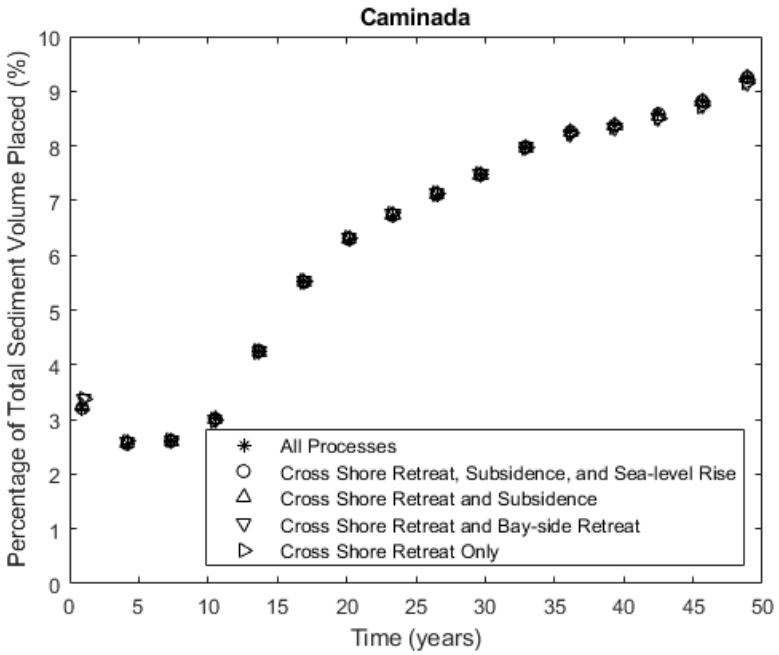

Figure 26. Restoration frequency for Caminada Headland for model simulations including different combinations of processes, including: (1) cross-shore retreat only; (2) cross-shore retreat and bayside retreat; (3) cross-shore retreat and subsidence; (4) cross-shore retreat, subsidence, and SLR; and (5) all processes activated. Sediment volumes are normalized by the total sediment volume placed.

3.3 MODEL INITIAL CONDITIONS

An initial DEM was provided to CPRA by USGS. This DEM was a preliminary version of the update to the northern Gulf of Mexico component of the Coastal National Elevation Dataset at a 10 m resolution. Upon detailed inspection of the DEM, several elevation offsets of at least 1 m were found. To correct for these offsets, other coastal elevation data sets were used. Along the Central Coast (Isles Dernieres to Barataria regions), the 2010s bathymetry surface was used (Applied Coastal Engineering, Inc., 2020), and the initial DEM from USGS was used for the topography. Along the Chandeleurs (Breton to Chandeleurs regions), 2015 topography and bathymetry from BICM2 was used (Stalk et al., 2017), and the initial DEM from USGS was used to fill gaps offshore and in the back bay. Initial ICM-BI profiles were extracted from this merged dataset and run through a one-year simulation to identify restoration units (barrier islands and headlands) that were at or above the threshold for auto-restoration. In some cases (e.g., Whiskey Island, Shell Island East and Shell Island West), these restoration units had undergone actual restoration subsequent to the timing of data collection used to compile the DEM.

The ICM-BI model domain initial condition for ICM production runs was modified to add restoration via a monitored auto-restoration process for those units that would otherwise auto-restore during the first year (Table 2). This process allowed refinement of the placement of the template in the case of degraded barrier islands that required manual quality control of the cross-shore positioning of the applied template.

Table 2. Restoration units that were restored through a monitored auto-restoration process to modify the initial condition DEM for the ICM-BI model domain.

Model Region	Units Restored within the Initial DEM
Isles Dernieres	East/Trinity, Whiskey Island
Timbalier	Timbalier
Caminada	West Belle Pass
Barataria	Scofield, Pelican, Shell Island, Chaland, East Grand Terre, and West Grand Terre
Breton	Breton Island
Chandeleur	North Chandeleur and South Chandeleur Units

3.4 MODEL ASSESSMENT

Model assessment consisted of two components: (1) hindcasting for portions of the coast to assess model performance against historical data, and (2) conducting standalone simulations for the 50-year period of 2015–2065 to parameterize and assess formulations related to auto-restoration and the modulation of cross-shore retreat rates with RSLR.

Hindcast simulations for selected sections of the coast were conducted and compared to historical seafloor change and shoreline retreat trends (Figure 27–Figure 30). Assessment runs were conducted for two of the regions: Caminada (1930s to 1980s) and Chandeleurs (1920s to 2000s). These areas of the coast were selected to represent spatial variability in the model domain, with time periods of validation based on available data. For the assessment runs, the cross-shore retreat rates as calculated above for the time period of 1920s to 2010s were used for the Gulfside shoreline and shoreface retreat. Bayside retreat rates from the 2017 Coastal Master Plan were extracted at the grid profiles and used to predict marsh shoreline erosion. Historical RSLR was obtained from the NOAA Grand Isle tide gauge as 9.13 mm/year (NOAA, 2020). This value includes both subsidence and eustatic SLR, which are separated within the model. To calculate these values, eustatic SLR was taken from the Pensacola tide gauge (NOAA, 2020a) as 2.45 mm/yr and subtracted from the Grand Isle RSLR to obtain a subsidence rate of 6.67 mm/yr (Penland & Ramsey, 1990; Kolker et al., 2011). Auto-restoration was not included in hindcast simulations.

To assess model stability, simulations were conducted over the period of 2015–2065 from the ICM-BI initial condition DEM described above. All model formulations were included in the simulations, including cross-shore retreat with modulation by SLR, bayside edge retreat, subsidence, accretion in marsh areas, and auto-restoration. The same subsidence rate (6.67 mm/yr), cross-shore retreat rates, and bayside erosions rates used for the hindcast were used in the prediction. Because the model was running standalone without water level inputs from the ICM, a proxy time series of water level was used based an approximation of a "high" SLR scenario evaluated for the 2017 Coastal Master Plan. The initial MHW was set at 0.16 m, with a eustatic SLR rate of 16.7 mm/yr. The threshold for auto-restoration was set at 10% of profiles falling below the restoration threshold, with the critical width of the barrier island set to 75% of the restoration template for that location. Simulations were conducted for all six of the coastal regions and confirmed that: (1) model simulations completed without error over the 50-year simulation period; and (2) output files were generated correctly.

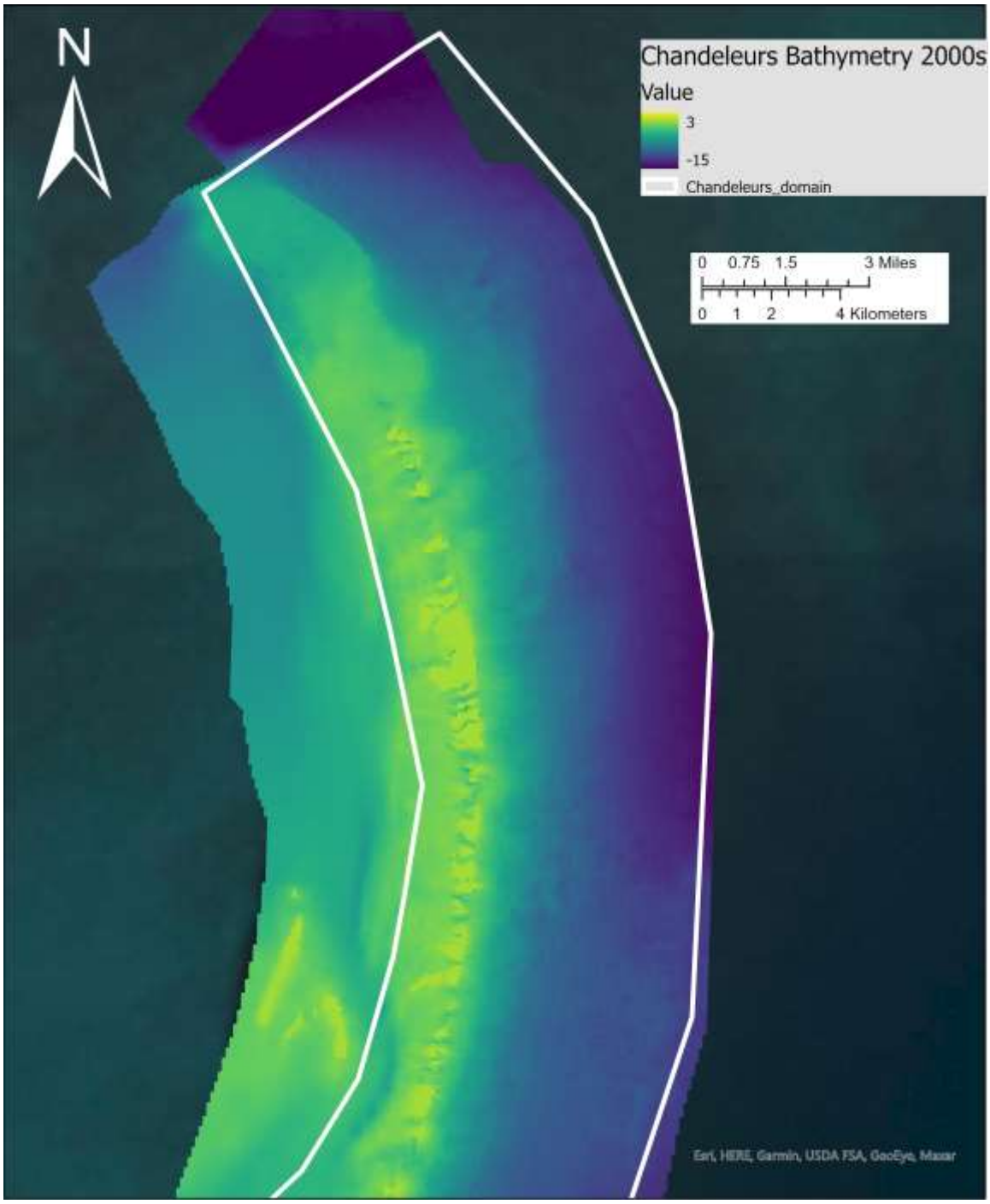

Figure 27. Topography and bathymetry data for the 2000s time period used to compare with the model hincast from 1920 to 2006.

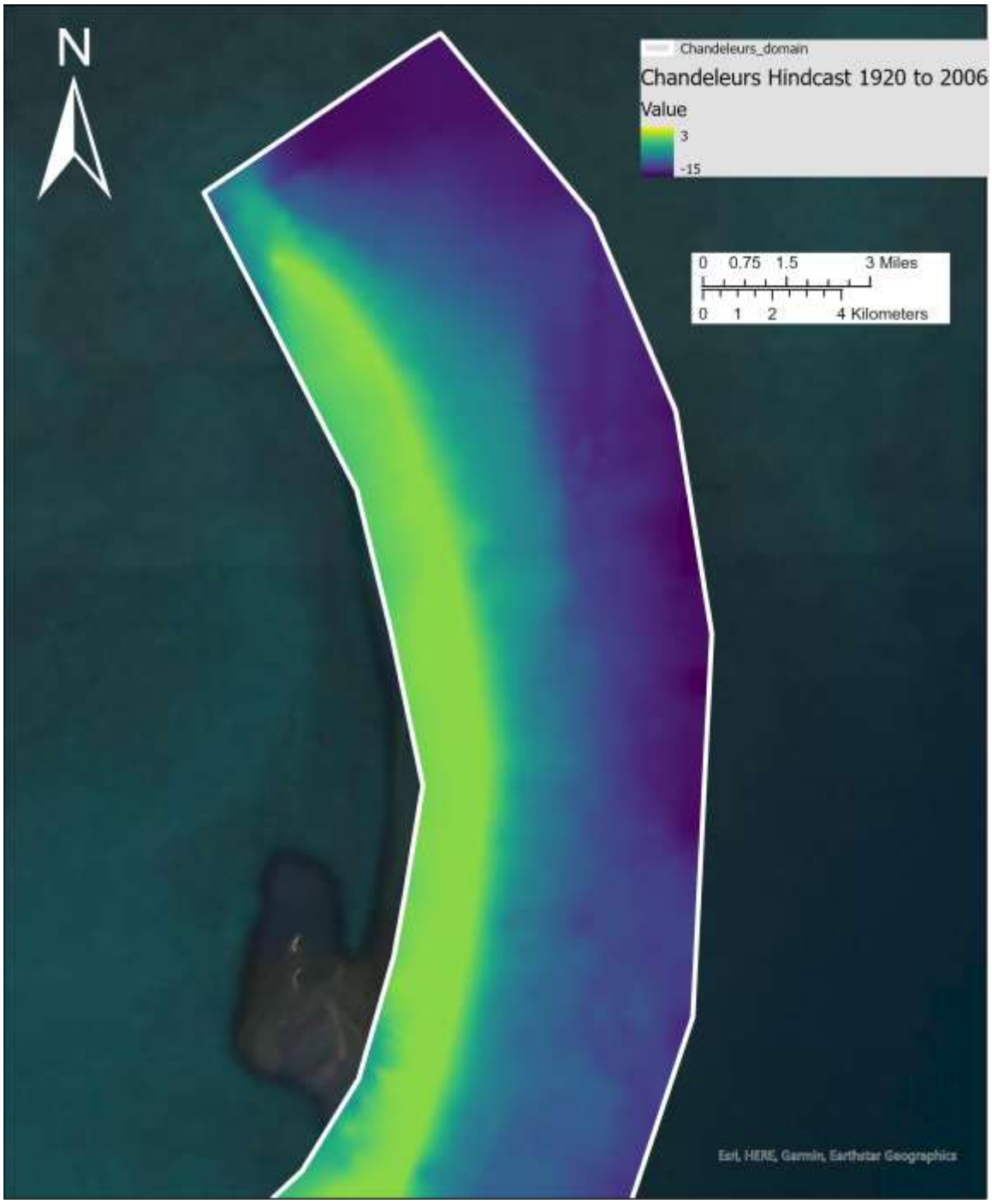

Figure 28. Model hindcast for the Chandeleurs region from 1920 to 2006. The model grid transects were interpolated to a 30 m surface.

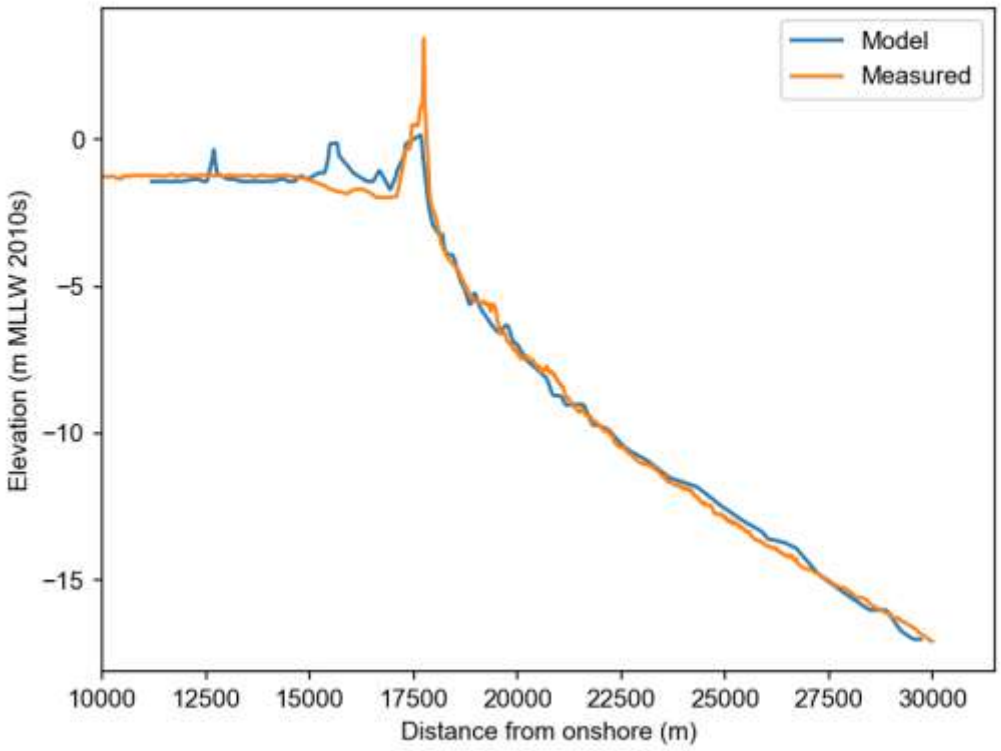

Figure 29. Transect 514 from the Caminada region showing a comparison of the modeled results from the period 1980 to 2015 to the measured 2010s topobathy. Note that the 1980 initial condition data set (from List et al., 1994) was only bathymetry with no topographic data (subaerial barrier island was not captured by the dataset).

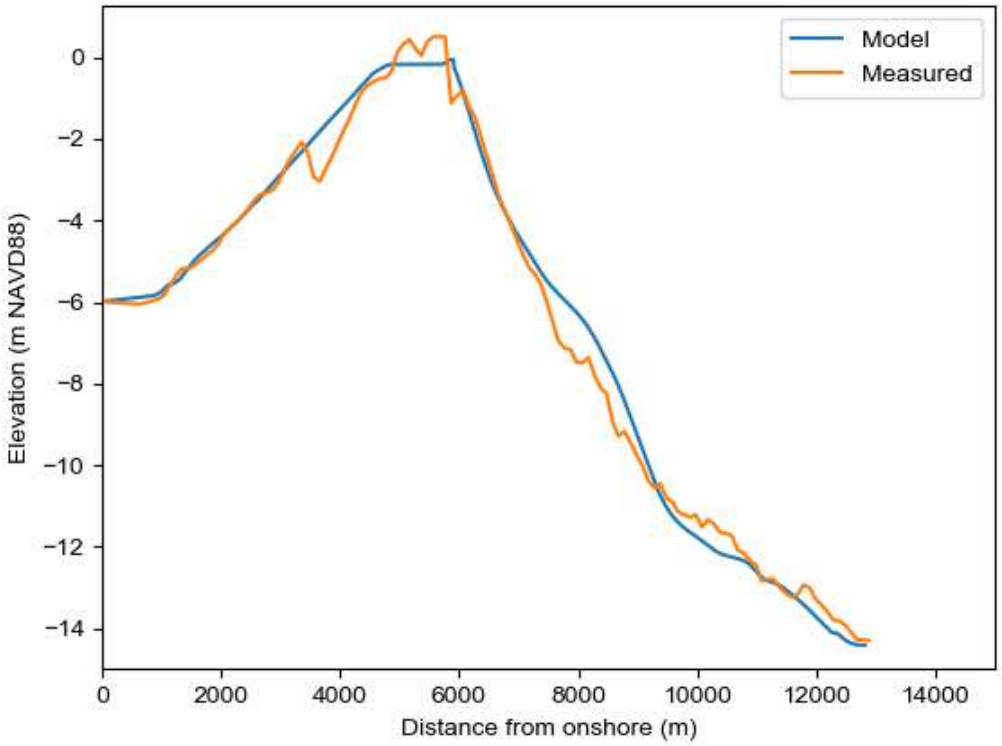

Figure 30. Transect 804 from the Chandeleurs region showing the modeled results from the period 1920 to 2006 and the measured topobathy from the 2000s.

4.0 FUTURE MODEL RECOMMENDATIONS

The ICM-Barrier Islands Improvement Team previously proposed an extension of the ICM-BI modeling approach to incorporate a more process-based approach to modeling barrier islands, headlands, and adjacent shorefaces (Georgiou et al., 2019). Here, the team identified several additional areas of potential improvement for future Coastal Master Plan modeling efforts. These include:

1. Incorporation of ICM-BI within the ICM

In the current model formulation, ICM-BI has its own grid and set of input files. Each year that the ICM is run, it writes a water level input file and runs ICM-BI, which then generates its output for the end of the year and passes control back to the ICM. These output files from a given year provide the inputs to ICM-BI for the subsequent year. This compartmentalized approach provides the benefit that ICM-BI can be run independently of the ICM. However, the input/output (I/O) components of ICM-BI account for ~50% of the computational model run time for a one-year run. A significant potential improvement in model run time is to incorporate the ICM-BI within the ICM to reduce I/O requirements. This will eliminate the need to read in input files, including the memory-intensive grid files, after the first year the model is run. In addition, it would reduce the number of output files that are written by eliminating the need for files that are solely required for reinitializing the model (i.e., location of the edge between the barrier islands and marsh islands, location of the restoration template location for headlands).

2. Modification of the linkage between ICM-BI and the rest of the ICM to remove the requirement for a fixed grid

Because the fixed grid domain for ICM-BI to provide output to ICM must extend far enough toward the mainland to allow for barrier island transgression and headland erosion under the highest rates of RSLR, it includes marsh islands and a portion of the headland marsh that would otherwise be included in ICM-Morph. The ICM-BI does not include marsh accretion processes and instead uses empirical formulations based on an assumption that marshes will keep pace with RSLR, limiting the capacity of the model to predict evolution of these areas. Modifying the workflow to allow for the migrating ICM-BI domain to be used to update (only) the regions of the ICM-Morph domain where the barrier islands and headlands are located at a given point in time would allow ICM-Morph and ICM-LAVegMod to produce more accurate predictions of marsh islands. If done in conjunction with direct incorporation of ICM-BI with ICM (recommendation 1), the formulations for marsh accretion could also potentially be

used for more accurate modeling of the back-barrier marshes that are an inherent component of the ICM-BI domain.

3. Integration between ICM-BI and ICM-Morph to better represent processes governing ebb tidal delta morphology and dynamics and interactions with inlets and adjacent shorelines

The integration of tidal prism changes and subsequent feedback to update the inlet cross-sectional area of Type 1 links (inlets) in ICM-Hydro is a substantial improvement in the modeling framework. However, the morphology of tidal inlets as well as the adjacent barrier island shoreline and shoreface depends on dynamic interaction of inlets with their proximal environments such as ebb and flood tidal deltas. The evolution of ebb/tidal shoal morphology can affect sediment bypassing to downdrift shorelines. In addition, expanding ebb tidal deltas can encroach into the adjacent barrier island shoreface. In future iterations of Coastal Master Plan modeling, it is recommended that a workflow be established for more seamless integration of ICM-BI, ICM-Morph, and ICM-Hydro. For example, velocity fields from ICM-Hydro can be used to predict inlet stability and evolution. In addition, theoretical and empirical formulations should be used to establish the footprint and size of the expanding ebb delta with feedback to ICM-BI to adjust or modulate retreat rates (historical or calculated) as a result of this process.

REFERENCES

Applied Coastal Engineering, Inc. (2020). Louisiana Operational Sediment Budget: Raccoon Point to Sandy Point, 1985-89 to 2013-16 (p. 182). Applied Coastal Engineering, Inc. Prepared for Louisiana Coastal Protection and Restoration Authority. https://cims.coastal.louisiana.gov/RecordDetail.aspx?Root=0&sid=23926

Applied Coastal Engineering, Inc., & CDM Smith. (2018). Louisiana Barrier Island Comprehensive Monitoring Program (BICM): Phase 2 – Updated Shoreline Compilation and Change Assessment, 1880s to 2015 [Louisiana Coastal Protection and Restoration Authority].

Beasley, B., Georgiou, I., Miner, M., & Byrnes, M. (2019). Coupled Barrier System Shoreline and Shoreface Dynamics, Louisiana, USA. Proceedings of the 9th International Symposium on Coastal Engineering and Science of Coastal Sediment Processes (pp. 172–186). Presented at the Coastal Sediments 2019, St. Petersburg, Florida.

Beasley, B. S. (2018). Coupled Barrier Island Shoreline and Shoreface Dynamics (Master's Thesis). University of New Orleans, New Orleans, LA.

Coastal Engineering Consultants, Inc. (2015). Barrier Island/Barrier Headland Restoration Design Template Development Technical Memorandum. CEC File No. 13.084.

Coastal Engineering Consultants Inc. (2019). *Terrebonne Basin Barrier Island and Beach nourishment/West Belle Headland Restoration Construction Plans* (No. TE-143/TE-118) (p. 101). Coastal Restoration and Protection Authority.

D'Alpaos, Andrea, Stefano Lanzoni, Marco Marani, and Andrea Rinaldo. "On the O'Brien–Jarrett–Marchi law." Rendiconti Lincei 20, no. 3 (2009): 225-236.

FitzGerald, D. M., Kulp, M. A., Hughes, Z. J., Georgiou, I. Y., Miner, M. D., Penland, S., & Howes, N. C. (2007). Impacts of rising sea level to backbarrier wetlands, tidal inlets, and barrier islands: Barataria coast, Louisiana. Coastal Sediments '07, 1179–1192. https://doi.org/10.1061/40926(239)91

FitzGerald, D. M., & Miner, M. D. (2013). Tidal inlets and lagoons along siliciclastic barrier coasts. In *Treatise on Geomorphology* (John F. Shroder, Vol. 10, pp. 149–165). http://dx.doi.org/10.1016/B978-0-12-374739-6.00278-5.

FitzGerald, D., Penland, S., & Nummedal, D. (1984). Changes in tidal inlet geometry due to backbarrier filling: East Friesian Islands, West Germany. Shore and Beach, 52(4), 2–8.

Gehrels, W. R., Belknap, D. F., Pearce, B. R., & Gong, B. (1995). Modeling the contribution of M2 tidal amplification to the Holocene rise of mean high water in the Gulf of Maine and the Bay of Fundy. Marine Geology, 124(1-4), 71-85.

Georgiou, I., Foster-Martinez, M., Fitzpatrick, C., Jarrell, E., Bridgeman, J., Lee, D., Miner, M., Dalyander, S., Dong, Z. (2019). ICM-Barrier Islands Model Team Improvement, Technical Report. 29 p.

Hayes, M. O. (1980). General morphology and sediment patterns in tidal inlets. Sedimentary Geology, 26(1–3), 139–156. https://doi.org/10.1016/0037-0738(80)90009-3

Howes, N. C. (2009). The impact of wetland loss on inlet morphology and tidal range within Barataria Bay, Louisiana. (Master's Thesis). Boston University. Boston, MA.

Hughes, Z., Weathers, D., Georgiou, I., FitzGerald, D., & Kulp, M. (2012). Appendix D-3: Barrier shoreline morphology model technical report. Louisiana's Comprehensive Master Plan for a Sustainable Coast, 1–40.

ICM-Barrier Islands Model Improvement Team - Georgiou, I., Foster-Martinez, M., Fitzpatrick, C., Jarrell, E., Bridgeman, J., Lee, D., Miner, M., Dalyander, S., Dong, Z. (2019).

Jarrett, J. T. (1976). Tidal prism-inlet area relationships (Vol. 3). US Department of Defense, Department of the Army, Corps of Engineers, Experiment Station.

Kindinger, J. L., Buster, N. A., Flocks, J. G., Bernier, J. C., & Kulp, M. A. (2013). Louisiana Barrier Island Comprehensive Monitoring (BICM) Program Summary Report: Data and Analyses 2006 through 2010 (Open-File Report No. 2013–1083; Open-File Report, p. 86). U. S. Geological Survey.

Kolker, A.S., Allison, M.A., & Hameed, S. (2011). An evaluation of subsidence rates and sea-level variability in the northern Gulf of Mexico. *Geophysical Research Letters 38*, L21404.

Levin, D. R., 1993, Tidal inlet evolution in the Mississippi River delta plain: Journal of Coastal Research, v. 9, no. 2, p. 462 –480.

List, J. H., Jaffe, B. E., Sallenger Jr, A. H., Williams, S. J., McBride, R. A., & Penland, S. (1994). Louisiana barrier island erosion study; atlas of sea-floor changes from 1878 to 1989 (No. 2150-B).

McCorquodale, J. A., Meselhe, E. A., Rodrigue, M. D., Schindler, J., & White, E. D. (2017). 2017 Coastal Master Plan: Attachment C3-22.1: ICM-hydro flow calculations (Louisiana's Comprehensive Master Plan for a Sustainable Coast, pp. 1–21) [Version Final]. Coastal Protection and Restoration Authority. http://coastal.la.gov/our-plan/2017-coastal-master-plan/

Miner, M. D., Kulp, M. A., FitzGerald, D. M., Flocks, J. G., & Weathers, H. D. (2009a). Delta lobe degradation and hurricane impacts governing large-scale coastal behavior, South-central Louisiana, USA. Geo-Marine Letters, 29(6), 441–453. https://doi.org/10.1007/s00367-009-0156-4.

Miner, M., Kulp, M., Weathers, H., & Flocks, J. (2009b). Historical (1869–2007) sea floor evolution and sediment dynamics along the Chandeleur Islands. In Lavoie, D., Sand Resources, Regional Geology, and Coastal Processes of the Chandeleur Islands Coastal System—an Evaluation of the Breton National Wildlife Refuge, (p. 47–74).US Geological Survey Scientific Investigations Report, 5252.

Nienhuis, J. H., & Lorenzo-Trueba, J. (2019). Simulating barrier island response to sea-level rise with the barrier island and inlet environment (BRIE) model v1.0. *Geoscientific Model Development Discussions*, 1–33.

NOAA. (2020). National Oceanic and Atmospheric Administration Grand Isle tide gauge. https://tidesandcurrents.noaa.gov/sltrends/sltrends_station.shtml?id=8761724

NOAA (2020a). National Oceanic and Atmospheric Administration Pensacola tide gauge. https://tidesandcurrents.noaa.gov/sltrends/sltrends_station.shtml?id=8729840

O'Brien, M. P. (1966). Equilibrium flow areas of tidal inlets on sandy coasts. In Coastal Engineering 1966 (pp. 676–686). U.S. Army Corps of Engineers. https://doi.org/10.1061/9780872620087.039

Penland, S., Boyd, R., & Suter, J. R. (1988). Transgressive depositional systems of the Mississippi delta plain: A model for barrier shoreline and shelf sand development. Journal of Sedimentary Petrology, 58(6), 932–949. https://doi.org/10.1306/212F8EC2-2B24-11D7-8648000102C1865D

Penland, S., & Ramsey, K.E. (1990). Relative sea-level rise in Louisiana and the Gulf of Mexico: 1908-1988. *Journal of Coastal Research* 6(2), 323-342.

Poff, M., Georgiou, I., Kulp, M., Leadon, M., Thomson, G., & Walstra, D.J.R. (2017). 2017 Coastal Master Plan Modeling: Attachment C3-4: Barrier Island Model Development (BIMODE). Baton Rouge, Louisiana: Coastal Protection and Restoration Authority, 128 p.

Ranasinghe, R., Duong, T. M., Uhlenbrook, S., Roelvink, D., & Stive, M. (2013). Climate-change impact assessment for inlet-interrupted coastlines. Nature Climate Change, 3(1), 83–87. https://doi.org/10.1038/nclimate1664

Stalk, C.A., DeWitt, N.T., Bernier, J.C., Kindinger, J.G., Flocks, J.G., Miselis, J.L., Locker, S.D., Kelso, K.W., and Tuten, T.M. (2017). Coastal single-beam bathymetry data collected in 2015 from the Chandeleur Islands, Louisiana: U.S. Geological Survey Data Series 1039, https://doi.org/10.3133/ds1039.

White, E.D., Meselhe, E, McCorquodale, A, Couvillion, B, Dong, Z, Duke-Sylvester, S.M., & Wang, Y. (2017). 2017 Coastal Master Plan: Attachment C2-22: Integrated Compartment Model (ICM) Development. Version Final. (pp.1-49). Baton Rouge, Louisiana: Coastal Protection and Restoration Authority

APPENDIX 1: RESTORATION UNIT DELINEATION AND RESTORATION TEMPLATE SOURCES

ID	Unit Name	Unit Type	Template Source	Restoration Template
1	Raccoon Island	n/a	n/a	Raccoon Island is the terminus of a long-shore transport cell that has been stabilized using rock breakwaters to limit erosion and protect a rookery on the island. Sediment placement at the island has historically been through marsh creation along the back barrier. Cross-shore retreat within the ICM-BI model has been set to zero for this island and auto-restoration turned off to be consistent with this management strategy, which does not include beach and dune fill placement.
2	Whiskey Island	Barrier Island	Caillou Lake Headland Restoration (TE-100)	Restoration at Whiskey Island was conducted during two phases – a marsh restoration in 2009 (TE-50) and a large-scale restoration of the beach, dune, and remaining portions of the back-barrier marsh in 2018 (TE-100). Template C from the TE-100 project was used as the template within the ICM-BI model. https://cims.coastal.louisiana.gov/outreach/projects/ProjectView?projID=TE-0050 https://cims.coastal.louisiana.gov/outreach/projects/ProjectView?projID=TE-0100

ID	Unit Name	Unit Type	Template Source	Restoration Template
3	East/ Trinity Island	Barrier Island	Terrebonne Basin Barrier Island and Beach Nourishment/West Belle Headland Restoration Project (TE-143, TE-118; planned)	The restoration template used for East/Trinity Island is the restoration template designed under TE-143 for application to Timbalier Island. The back-barrier marsh of the template was extended to 1300' to encompass the existing marsh for the island under the assumption that future restoration action would preserve the back-barrier marsh. https://cims.coastal.louisiana.gov/outreach/projects/ProjectView?projID=TE-0143
4	Timbalier Island	Barrier Island	Terrebonne Basin Barrier Island and Beach Nourishment/West Belle Headland Restoration Project (TE-143, TE-118; planned)	The restoration template used for Timbalier Island is the restoration template designed under TE-143. The back-barrier marsh of the template was extended to 1300' to encompass the existing marsh for the island under the assumption that future restoration action would preserve the back-barrier marsh. https://cims.coastal.louisiana.gov/outreach/projects/ProjectView?projID=TE-0143
5	East Timbalier, Casse-tete, and Calumet	n/a	n/a	Restoration of East Timbalier Island was excluded during a recent round of restoration efforts and plans have not been developed for Casse-tete and Calumet, therefore these units were not included in auto-restoration. Cross-shore retreat was applied to the shoreface along East Timbalier.
6	West Belle Pass	Headland, managed retreat	Terrebonne Basin Barrier Island and Beach	The model uses the restoration template designed under TE-143 for the West Belle Pass restoration. The template used is designated "B" in the design report and includes restoration of the back-barrier marsh.

ID	Unit Name	Unit Type	Template Source	Restoration Template
			Nourishment/West Belle Headland Restoration Project (TE-143)	https://cims.coastal.louisiana.gov/outreach/projects/ProjectView?projID=TE-0143
7	Caminada Headland	Headland, "hold the line" for Port Fourchon, otherwise managed retreat	Caminada Headland Beach and Dune Restoration (BA-0045)	The template used for the entire reach of the Caminada Headland restoration unit is design "A" from the BA-0045 restoration project. https://cims.coastal.louisiana.gov/outreach/projects/ProjectView?projID=BA-0045
8	Grand Isle	Special case: barrier island keeps pace with RSLR.	n/a	Grand Isle has been stabilized through the use of rock jetties and seawalls, therefore the managed transgression model will not accurately capture the future trajectory of this island. For the ICM-BI model, cross-shore retreat has been set to zero. In lieu of auto-restoration, the subaerial footprint of the island is raised to keep pace with RSLR. Note, while this configuration captures the assumption that Grand Isle will be maintained in place and not transgress or retreat, the model cannot accurately predict changes to, for example, the shoreface that may occur despite the presence of the rock structures.
9	West Grand Terre	Barrier Island	West Grand Terre Beach Nourishment and Stabilization (BA-197)	The template used for West Grand Terre is template "C" from the planned BA-197 restoration project. https://cims.coastal.louisiana.gov/outreach/projects/ProjectView?projID=BA-0197
10	East Grand	Barrier Island	West Grand Terre Beach	The same template used for West Grand Terre, template "C" from the planned BA-197 restoration

ID	Unit Name	Unit Type	Template Source	Restoration Template
	Terre		Nourishment and Stabilization (BA-197)	project, was applied for restoration of East Grand Terre. This template was chosen as being representative of expected future restoration action at East Grand Terre. https://cims.coastal.louisiana.gov/outreach/projects/ProjectView?projID=BA-0197
11	Grand Pierre	Barrier Island	West Grand Terre Beach Nourishment and Stabilization (BA-197)	The same template used for West Grand Terre, template "C" from the planned BA-197 restoration project, was applied for restoration of East Grand Terre. This template was chosen as being representative of expected future restoration action at Grand Pierre. https://cims.coastal.louisiana.gov/outreach/projects/ProjectView?projID=BA-0197
12	Chaland Headland	Headland, managed retreat	Barataria Barrier Island Complex: Pelican Island and Pass La Mer to Chaland Pass Restoration (BA-038)	The template used for the Chaland Headland restoration unit was developed for the BA-038 restoration project of a portion of this region. https://cims.coastal.louisiana.gov/outreach/projects/ProjectView?projID=BA-0038
13	Shell Island	Barrier Island	Barataria Barrier Island Complex: Pelican Island and Pass La Mer to Chaland Pass Restoration (BA-038)	The template developed for the BA-038 restoration project within the Barataria Barrier Island Complex was used for Shell Island. This template was chosen because prior restoration at Shell Island was an emergency berm constructed as part of the Deepwater Horizon Oil Spill response and was not designed as part of restoration planning. https://cims.coastal.louisiana.gov/outreach/projects/ProjectView?projID=BA-0038
14	Pelican	Barrier Island	Barataria	The template developed for the BA-038 restoration

ID	Unit Name	Unit Type	Template Source	Restoration Template
	Island		Barrier Island Complex: Pelican Island and Pass La Mer to Chaland Pass Restoration (BA-038)	project within the Barataria Barrier Island Complex was used for Pelican Island. This template was chosen because prior restoration at Pelican Island was an emergency berm constructed as part of the Deepwater Horizon Oil Spill response and was not designed as part of restoration planning. https://cims.coastal.louisiana.gov/outreach/projects/ProjectView?projID=BA-0038
15	Scofield Island	Barrier Island	Barataria Barrier Island Complex: Pelican Island and Pass La Mer to Chaland Pass Restoration (BA-038)	The template developed for the BA-038 restoration project within the Barataria Barrier Island Complex was used for Scofield Island. This template was chosen because prior restoration at Scofield Island was an emergency berm constructed as part of the Deepwater Horizon Oil Spill response and was not designed as part of restoration planning. https://cims.coastal.louisiana.gov/outreach/projects/ProjectView?projID=BA-0038
16	Breton Island	Barrier Island	Louisiana Outer Coast Restoration Project – North Breton (USFWS)	The Geologic Form and Function (GEFF) template developed for the USFWS-led restoration of North Breton Island was used as the template. https://www.doi.gov/restoration/deepwater-horizon-n-breton-island-restoration
17	South Chandeleurs	Barrier Island	Barataria Barrier Island Complex: Pelican Island and Pass La Mer to Chaland Pass Restoration (BA-038)	The template developed for the BA-038 restoration project within the Barataria Barrier Island Complex was used for the Chandeleur Islands. This template was chosen because prior restoration in the Chandeleurs was an emergency berm constructed as part of the Deepwater Horizon Oil Spill response and was not designed as part of restoration planning. https://cims.coastal.louisiana.gov/outreach/projects/ProjectView?projID=BA-0038
18	North	Barrier Island	Barataria	The template developed for the BA-038 restoration

ID	Unit Name	Unit Type	Template Source	Restoration Template
	Chandeleurs		Barrier Island Complex: Pelican Island and Pass La Mer to Chaland Pass Restoration (BA-038)	project within the Barataria Barrier Island Complex was used for the Chandeleur Islands. This template was chosen because prior restoration in the Chandeleurs was an emergency berm constructed as part of the Deepwater Horizon Oil Spill response and was not designed as part of restoration planning. https://cims.coastal.louisiana.gov/outreach/projects/ProjectView?projID=BA-0038